UNIVERSITÀ
DEGLI STUDI
DI PADOVA

Sede Amministrativa: Università degli Studi di Padova

Dipartimento di Scienze Biomediche

SCUOLA DI DOTTORATO DI RICERCA IN: **BIOSCIENZE E BIOTECNOLOGIE**

INDIRIZZO: **BIOCHIMICA E BIOFISICA**

CICLO XXV

Investigating The Role Of The Cellular Prion Protein In Ca^{2+} Metabolism And Alzheimer's Disease

Direttore della Scuola : Ch.mo Prof. Giuseppe Zanotti

Coordinatore d'indirizzo : Ch.mo Prof. ssa Maria Catia Sorgato

Supervisore : Ch.mo Prof. ssa Maria Catia Sorgato

Dottorando : Angela Castellani

31 Gennaio 2013

INDEX

ABSTRACT

The cellular prion protein (PrP^C) is a highly conserved cell-surface glycoprotein expressed in almost all mammalian tissues, in particular in the central nervous systems. The bad reputation acquired by PrP^C originates from its capacity to convert into an aberrant conformer (PrP^{Sc}), which is the major component of the prion, the unconventional infectious particle causing fatal neurodegenerative disorders, known as prion diseases. Both the mechanism of prion related neurodegeneration and the physiologic role of PrP^C are still unknown. However, use of animal and cell models has underscored a number of putative functions for PrP^C, suggesting that it could serve in cell adhesion, migration, proliferation and differentiation, possibly by interacting with extracellular partners, and/or by taking part in multi-component signaling complexes at the cell surface. An intriguing hypothesis, based on increasing amounts of data that may explain the multifaceted behavior of PrP^C, entails that the protein is involved in the regulation of Ca^{2+} homeostasis

One major part of the present thesis deals with a close investigation of the alleged regulation of Ca^2 homeostasis by PrP^C. This study was carried out by monitoring local Ca^{2+} movements in primary cultures of cerebellar granule neurons (CGN) – obtained from PrP-knockout mice and transgenic PrP^C-expressing mice – subjected to various stimuli. Measurements of Ca^{2+} fluxes in different cell domains were accomplished using the Ca^{2+}- sensitive photo-protein aequorin genetically targeted to different cell domains (plasma membrane, cytosol, lumen of the endoplasmic reticulum and mitochondrial matrix). We found that, with respect to PrP^C-expressing neurons, the absence of PrP^C caused alterations of local Ca^{2+} movements, indicating that PrP^C may be part of the cellular system(s) deputed to avoid toxic neuronal Ca^{2+} accumulation. As for the molecular mechanisms by which PrP^C controls Ca^{2+} homeostasis, we found that this could be accomplished through the modulation of $p59^{Fyn}$- and p42/p44-ERK-dependent signaling pathways.

Another topic studied in this thesis stemmed from recent reports indicating that PrP^C could acts as a high-affinity receptor for amyloid-β (Aβ) peptides implicated in Alzheimer's disease. The possibility that PrP^C-Aβ interactions may impair synaptic plasticity is, however, still highly debated. Thus, given that Ca^{2+} is intimately related to synaptic plasticity, we investigated whether Aβ peptides affected Ca^{2+} metabolism in a PrP^C-dependent manner using the above-mentioned strategies and cell paradigms. The obtained results showed that interactions

between PrP^{C} and Aβ oligomers may cause Ca^{2+} accumulation following activation of store-operated Ca^{2+} entry, and that this may occur *via* a PrP^{C}-dependent activation of $p59^{Fyn}$ kinase.

SINOSSI

La proteina prionica cellulare (PrP^{C}) è una glicoproteina di membrana altamente conservata nei mammiferi ed espressa abbondantemente nel sistema nervoso centrale. La cattiva reputazione attribuita a questa proteina nasce dalla sua capacità di convertirsi in un'isoforma conformazionale patologica (PrP^{Sc}), che è la componente principale del prione. Il prione è l'agente eziologico di malattie neurodegenerative fatali per l'uomo e per gli altri animali conosciute come malattie prioniche (Prusiner, 1998). Tuttavia rimangono ancora da capire sia il meccanismo attraverso cui PrP^{Sc} causa neurodegenerazione, sia la funzione fisiologica di PrP^{C}.

L'uso di svariati modelli animali e cellulari ha attribuito numerose funzioni a PrP^{C}, suggerendo che essa sia coinvolta in numerosi processi cellulari, quali adesione, migrazione, proliferazione e differenziamento, mediante interazioni con partner extracellulari e di membrana, e/o partecipando a vie di segnalazione cellulare. Un'ipotesi plausibile che potrebbe spiegare questo comportamento poliedrico, è che PrP^{C} sia coinvolta nella regolazione dell'omeostasi del Ca^{2+}, il secondo messaggero che è anch'esso in grado di controllare un gran numero di processi fisio-patologici che vanno dalla sopravvivenza alla morte della cellula.

Uno dei principali argomenti affrontati in questa tesi riguarda per l'appunto la possibile regolazione dell'omeostasi di Ca^{2+} da parte di PrP^{C}. Lo studio è stato condotto confrontando i flussi locali di Ca^{2+} in colture primarie di neuroni granulari cerebellari (NGC) ottenuti da topi privi di PrP^{C} o esprimenti la proteina, a seguito dell'applicazioni di stimoli opportuni. Per il monitoraggio del Ca^{2+} si è impiegata la sonda Ca^{2+}-sensibile equorina indirizzata a specifici comparti cellulari (membrana plasmatica, citosol, lume del reticolo endoplasmico e matrice mitocondriale). Si è trovato che, rispetto ai neuroni esprimenti la PrP^{C}, l'assenza della proteina comporta alterazioni dei flussi locali di Ca^{2+}, così suggerendo che PrP^{C} possa far parte dei sistemi che proteggono il neurone dall'accumulo tossico di Ca^{2+}. Per quanto riguarda i meccanismi molecolari attraverso cui PrP^{C} controlla l'omeostasi del Ca^{2+}, si è scoperto che questo potrebbe essere realizzato mediante la modulazione delle vie di segnalazione dipendenti dalle chinasi $p59^{Fyn}$ e p42/p44-ERK.

Un altro tema di studio oggetto di questa tesi si collega a dati recenti che hanno evidenziato come la PrP^{C} possa legare con alta affinità i peptidi Aβ implicati della malattia di Alzheimer. La possibilità che queste interazioni alterino la plasticità sinaptica è, tuttavia, molto dibattuta. Pertanto, dal momento che il Ca^{2+} è finemente coinvolto in questo processo, si è voluto esplorare se la presenza dei peptidi Aβ influisca sui flussi di Ca^{2+} in maniera dipendente da PrP^{C}.

A tal scopo si sono usate sia le strategie sia i modelli cellulari sopra descritti. I risultati ottenuti hanno dimostrato che l'incubazione dei neuroni con oligomeri Aβ causa l'influsso di Ca^{2+} nella cellula dopo attivazione della via nota come "store-operated Ca^{2+} entry", e che questo processo potrebbe avvenire mediante l'attivazione di $p59^{Fyn}$ dipendente da PrP^{C}.

ABBREVIATIONS

ACH, amyloid cascade hypothesis
AD, Alzheimer's disease
ADDLs, Aβ-derived diffusible ligands
AEQ, aequorin
AHP, after hyperpolarization
ALS, amyotrophic lateral sclerosis
AMPA, α-amino-3-hydroxy-5-methyl-4-isoxazolepropionic acid
AMPAR, AMPA receptor
APP, amyloid precursor protein
APP_{Swe}, human APP with the Swedish familial mutations
AraC, cytosine arabinoside
Aβ, amyloid-β
BSA, bovine serum albumin
BSE, bovine spongiform encephalopathy
cAMP, cyclic adenosine monophosphate
CGN, cerebellar granule neuron
CJD, Creutzfeldt-Jakob disease
CNS, central nervous system
COX8, subunit VIII of human cytochrome c oxidase
CWD, chronic wasting disease
ER, endoplasmic reticulum
ERK, extracellular signal-regulated kinase
FFI, fatal familial insomnia
GFAP, glial fibrillary acidic protein
GPI, glycosylphosphatidylinositol
GSS, Gerstmann-Sträussler-Scheinker syndrome
HA, hemagglutinin
HFIP, 1,1,1,3,3,3-hexafluoro-2-propanol
IB, isolation buffer
IP_3, inositol 1,4,5-triphosphate
KO, knock-out
Ln- γ1, laminin γ1 chain
LTD, long-term depression
LTP, long-term potentiation
mAb, monoclonal antibody
mGluR, metabotropic glutamate receptor
NFT, neurofibrillary tangle
NMDA, N-methyl-D-aspartic acid
NMDAR, NMDA receptor
ORF, open reading frame
pAb, polyclonal antibody

PBS, phosphate-buffered saline
PKA, protein kinase A
PKC, protein kinase C
PM, plasma membrane
PMCA, plasma membrane Ca^{2+}- ATPases
PMCA, protein misfolding cyclic amplification
PMD, protein misfolding disorder
PrP, prion protein
PVDF, polyvinylidene fluoride
RT, room temperature
SDS, sodium dodecyl-sulphate
SERCA, sarco-ER- Ca^{2+}- ATPases
SFK, Src family of tyrosine kinases
SNAP-25, synaptic-associated protein 25
SOCC, Store-Operated Ca^{2+} Channel
SOCE, store-operated Ca^{2+} entry
STI1, stress-inducible protein 1
STIM, Stromal Interaction Molecule
TBS, Tris-buffered saline
Tg, transgenic
TSE, Transmissible spongiform encephalopathie
WT, wild-type
α7nAChR, α7-nicotinic-acetylcholine receptor

1. INTRODUCTION

1.1 TRANSMISSIBLE SPONGIFORM ENCEPHALOPATHIES

Transmissible spongiform encephalopathies (TSEs), also known as prion diseases, are a group of rare and fatal infectious neurodegenerative disorders affecting humans and other mammalian species, which have an infectious, genetic, or sporadic nature (Prusiner, 1998). Affected individuals generally exhibit clinical symptoms of both cognitive (dementia) and motor (ataxia) dysfunctions (Aguzzi and Calella, 2009). Brain histopathology typically shows vacuolation (from which the term ‘‘spongiform’’), extensive astrogliosis, and deposition of protease-resistant protein aggregates (Colby and Prusiner, 2011). TSEs include Creutzfeldt-Jakob disease (CJD), Gerstmann-Sträussler-Scheinker syndrome (GSS), fatal familial insomnia (FFI) and kuru in humans; scrapie in sheep and goats; bovine spongiform encephalopathy (BSE, also known as “mad cow disease”) in cattle and chronic wasting disease (CWD) in cervids (Prusiner, 1998).

Despite CJD was first described at the beginning of last century by A. M. Jakob (Jakob, 1920), and the demonstration of scrapie transmissibility among sheep dates back to 1939 (Cullie and Chelle, 1939), TSE etiology remained elusive until the mid-60s when D. C. Gajdusek, after the seminal observation that kuru was probably infectious within New Guinea tribes practicing cannibalism, formally demonstrated transmissibility of kuru to monkeys (Gajdusek *et al.*, 1966), and of CJD to chimpanzees (Gibbs *et al.*, 1968). These and the previous studies on scrapie thus prompted investigators to unravel the nature of TSE infectious agent, which already at the time was considered of “unconventional” nature.

1.2 PRION

The *protein-only hypothesis*, conceiving that TSE infectious agent could be a protein capable of self-replication, was first formulated by Griffith (Griffith, 1967) following that the observations that the infectious material of scrapie was extremely resistant to procedures that normally destroy nucleic acids, e.g. high doses of ionizing radiation and UV (Alper *et al.*, 1967), and that the minimal molecular weight of the agent maintaining infectivity (around 2×10^5 Da) was too small to account for a virus or other types of micro-organisms (Alper *et al.*, 1966).

Little research was performed to test this hypothesis until in the early 80’s Prusiner and coworkers provided an impressive set of data after isolating the protease-resistant material (Bolton *et al.*, 1982), and demonstrating that the concentration of the protein in this material was proportional to the infectivity titer (Gabizon *et al.*, 1988). Prusiner thus named the agent

prion - for PRoteinaceus Infective ONly particle - and PrP^{Sc} (*Sc* for scrapie) its constitutive protein (Prusiner, 1982).

Nonetheless, for a long time the prion concept was considered heretical by the scientific community, rather skeptical to acknowledge that a protein could replicate itself and act as an infectious agent. A key step to bypass this "heresy" was provided by the identification of the gene encoding PrP^{Sc} (Oesch *et al.*, 1985) and the demonstration that the gene encoded a constitutive cellular protein expressed in mammals (named cellular prion protein, PrP^{C}) (Basler *et al.*, 1986). Today, we know that PrP^{C} and PrP^{Sc} have the same amino acid sequence (Stahl *et al.*, 1993) and posttranslational modifications and that they differ merely in terms of conformation: PrP^{C} structure contains 40% for α-helices and 3% of β-sheets, whereas a predominant content of β-sheets (45% over the 30% of α-helices) characterizes PrP^{Sc} (Pan *et al.*, 1993). Such conformational changes confer to PrP^{Sc} its typical physico-chemical and biological features, i.e., resistance to protease digestion (Prusiner *et al.*, 1984), insolubility in detergents (Meyer *et al.*, 1986), propensity to aggregate and to form fibrils and amyloids (Meyer *et al.*, 1986), and capacity to self-replicate (Bolton *et al.*, 1982). The crucial support to the prion as a self-propagating protein was finally provided by the demonstration that $Prnp^{0/0}$ mice (or PrP knockout (PrP-KO) mice without the PrP gene (PRPN)) were resistant to prion infection (Büeler *et al.*, 1992), and therefore that the presence of PrP^{C} is a prerequisite for the replication and propagation of PrP^{Sc}.

In 2001, *de novo* prions have been generated through the so-called protein misfolding cyclic amplification (PMCA) technology (Saborio *et al.*, 2001), by which - in analogy to PCR reactions - a small amount of template PrP^{Sc} could be amplified after sonicating PrP^{Sc}-containing material with non-infectious brain homogenate (Deleault *et al.*, 2007). Thus, PMCA provided a further demonstration that PrP^{Sc} acts as template for catalyzing the conversion of PrP^{C} in its misfolded, infectious conformer (Castilla *et al.*, 2005). Use of this technology has allowed accelerating research on the mechanism of formation and propagation of PrP^{Sc}, thereby revealing that PrP^{C}-PrP^{Sc} conversion could require one or more co-factor(s), provisionally designated protein X, and that, after the conversion process, PrP^{Sc} is incorporated in a growing polymer that, through an as yet unknown process, break into smaller template pieces that further amplify fibrils formation (Soto, 2011).

Prions are not nucleic acids, although it is now accepted that like nucleic acids they are subjected to mutations although of a different nature (Li *et al.*, 2010). That prion strains could exist was first formulated after observing that prions affecting distinct brain areas and giving rise to

characteristic clinical symptoms displayed typical biochemical signatures that reflected distinct conformations (Telling *et al.*, 1996; Prusiner, 1998). Recently, the capacity of prions to "adapt" to the environment in a Darwinian fashion has also been provided, a process that explains the long incubation time needed for prion of an animal species to adapt to another animal species before triggering morbidity (Li *et al.*, 2010).

Although the above-mentioned reports clearly demonstrate that PrP^{Sc} is an essential component of the prion and that it originates from PrP^{C}, other aspects of prion diseases remain to be clarified, in particular the mechanism by which prions trigger neurodegeneration. Indeed, while PrP^{Sc} accumulates relatively rapidly, neurodegeneration takes a much longer period of time to occur and is directly dependent on PrP^{C} expression in the brain (Sandberg *et al.*, 2011). In other words, it is still unclear whether TSE pathogenesis arises from a gain of PrP^{Sc} toxicity, or from a loss of PrP^{C} function, or from a combination of the two events.

Interestingly, recent research has shown that a "prion-like" propagation mechanism might also apply to misfolded proteins associated with the more common neurodegenerative diseases, such as Alzheimer's and Parkinson's disease, and amyotrophic lateral sclerosis (ALS) (Soto, 2003). These diseases, clustered as protein misfolding disorders (PMDs), although not yet showing infectious characters, could however have molecular mechanisms responsible for protein misfolding and aggregation similar to those assumed for TSEs, including the spread of neurotoxic protein assemblies throughout the nervous system (Soto, 2011). It is therefore feasible to hypothesize that future and complete understanding of the pathogenesis of prion diseases will also provide crucial insights into that of all PMDs.

1.3 CELLULAR PRION PROTEIN

1.3.1 GENE

PRNP, the chromosomal gene encoding PrP^{C}, is highly conserved in all mammals, being almost 90% of homology between the murine and human genes (Chesebro *et al.*, 1985) - and other species, such as birds (Gabriel *et al.*, 1992), reptiles (Simonic *et al.*, 2000), amphibians (Strumbo *et al.*, 2001), and fish (Oidtmann *et al.*, 2003).

The human PrP gene is present as a single copy and is located on the short arm of chromosome 20 (Sparkes *et al.*, 1986). It contains two exons (exon 1 and 2), separated by one intron. Exon 1, containing untranslated sequences, includes the promoter and termination sites, while exon 2 contains the whole open reading frame (ORF) that codes for PrP^{C} (Basler *et al.*, 1986; Lee *et al.*, 1998). The PrP promoter, lacking the TATA box, contains the CCAAT element and multiple copies

of the GC-rich repeat, a canonical binding site for the transcription factor Sp1 (McKnight and Tjian, 1986). Several evidences indicate that PRNP expression may also depend on the chromatin structure (Cabral *et al.*, 2002) and other transcription factors, e.g., AP2, MZF-1, MEF2 and MyT1 (Linden *et al.*, 2008).

PrP^C mRNA is constitutively present in the adult brain, and it is expressed by a tightly regulated process during brain development and neuronal differentiation (Chesebro *et al.*, 1985; Oesch *et al.*, 1985).

Several point mutations within PRNP are linked to TSE familial forms, which are supposed to de-stabilize the native PrP^C conformation and favor PrP^{Sc} formation (Aguzzi *et al.*, 2008). Familial CJD is caused by autosomal dominant insertions of octarepeats (see below) present in the N-terminus, or point mutations in the C-terminus between the second and the third helices (Owen *et al.*, 1989); familial GSS by mutations in the sequence of the central domain (Tateishi *et al.*, 1996), while FFI by the D178N aminoacid substitution, associated with the presence of methionine homozygosity (MM) at codon 129 (Goldfarb *et al.*, 1992). The importance of codon 129 polymorphism (methionine/valine) is strengthened by the observation that the same D178N mutation associated with 129MV results in a different disease phenotype, i.e. CJD (Zarranz *et al.*, 2005).

1.3.2 STRUCTURE AND METABOLISM

PrP^C is a glycoprotein expressed in almost all tissues of vertebrates, predominantly in the central nervous system (CNS) (Horiuchi *et al.*, 1995).

The protein structure consists of a flexible N-terminal tail and a globular C-terminus. In the latter there is a glycosylphosphatidylinositol (GPI) anchor that tethers PrP^C to the external surface of the plasma membrane (PM) in cholesterol- and sphingolipid-rich domains, called lipid rafts (Taylor and Hooper, 2006). The protein, however, may localize to non-raft domains especially during the clathrin-mediated endocytic process (Magalhaes *et al.*, 2002). As revealed by NMR studies, the C-terminus is highly structured, harboring two anti-parallel β-sheets and three α-helices (1-2-3) (Riek *et al.*, 1996; Zahn *et al.*, 2000). In contrast, the N-terminus lacks identifiable secondary structure at least under the used experimental conditions (Donne *et al.*, 1997).

PrP^C is synthesized in the rough endoplasmic reticulum (ER) and transits through the Golgi apparatus along the secretory way to the cell surface, during which is subjected to several posttranslational modifications (Béranger *et al.*, 2002; Stahl *et al.*, 1987). For example, the primary human sequence of 253 amino acids is reduced to the mature form of 208 amino acids,

after the removal of the first 22 amino acids and of the 231-253 amino acid stretch at the C-end. At the C-terminus, the GPI anchor is then attached, a disulfide bond connecting cysteines 179 and 214 is formed (Zahn *et al.*, 2000), while the dispensable glycosylation at Asn181 and Asn197 generates three – mono-, di- and un-glycosylated - PrP^C isoforms (Haraguchi *et al.*, 1989).

Notably, the N-terminal region contains a stretch of octapeptide repeats (PHGGGWGQ), capable to bind Cu^{2+} (Hornshaw *et al.*, 1995; Miura *et al.*, 1996). In addition to the cell Cu^{2+} metabolism, it has been proposed that binding to Cu^{2+} could affect the folding stability and structure of PrP^C N-terminus (Younan *et al.*, 2011).

1.3.3 FUNCTION

Albeit the identification of PrP^C dates back to more than 30 years ago (Basler *et al.*, 1986), the physiological function of the protein is still unknown. To this end, several lines of PrP-KO mice have been engineered (Büeler *et al.*, 1992; Manson *et al.*, 1994) that, although resistant to prion infection as previously mentioned, displayed a normal lifespan and no developmental or anatomical abnormalities (Büeler *et al.*, 1992; Manson *et al.*, 1994), except for mild neurophysiologic and behavioral deficits upon aging (Bremer *et al.*, 2010; Criado *et al.*, 2005; Nazor *et al.*, 2007). The lack of an overt phenotype has thus led to the hypothesis that compensatory mechanisms could mask the cellular effects of the PrP^C absence, which would become evident only under stress conditions. This was recently proved in both hematopoietic cells (Zhang *et al.*, 2006) and adult skeletal muscles (Stella *et al.*, 2010).

Over the years, many *in vivo* and *in vitro* strategies have been adopted to unravel the enigmatic function of PrP^C. These studies not only have revealed that PrP^C is involved in Cu^{2+} metabolism, but also suggested that it serves against oxidative injury and apoptosis and in cell adhesion, migration, proliferation and differentiation, following the interaction with several extracellular partners or by taking part in multicomponent signaling complexes at the cell surface (Aguzzi *et al.*, 2008; Linden *et al.*, 2008). A definitive answer is however still lacking. On the other hand, given the proposed plethora of function one may hypothesize that PrP^C could act as a scaffold protein in different cell surface complexes, and that specific signaling pathways get activated depending on the type and state of the cell, the expression level of PrP^C, and the local availability of extracellular and/or intracellular signalling molecules (Peggion *et al.*, 2011). In this framework, it has been proposed that the interaction of PrP^C with the stress-inducible protein 1 (STI1) leads to the capacity of PrP^C to bind to the α7-nicotinic-acetylcholine receptor (α7nAChR). The subsequent activation of the receptor could increase cytosolic Ca^{2+} levels thus triggering a

neuroprotective signal through the cyclic adenosine monophosphate (cAMP)/protein kinase A (PKA) pathway and neurite outgrowth through the extracellular signal-regulated kinase (ERK) pathway (Zanata *et al.*, 2002; Lopes *et al.*, 2005; Beraldo *et al.*, 2011).

Taken together, these and other observations all point to the notion that PrP^{C} has a beneficial role in the cell, thus favoring the possibility that, in prion disease, neurodegeneration is also due to a loss of PrP^{C} function (Nazor *et al.*, 2007) rather than to only the deadly gain of function by PrP^{Sc} (Aguzzi *et al.*, 2008).

1.4 PrP^{C} AND Ca^{2+} HOMEOSTASIS

Ca^{2+} is the major intracellular messenger responsible for many important cell processes, including gene regulation, hormone and neurotransmitter release, muscle contraction and, last but not the least, cell survival (Berridge *et al.*, 2003). At rest conditions, cytosolic Ca^{2+} concentrations are maintained at very low levels (0,1-0,5 μM) by buffer systems and by the action of pumps/transporters that extrude the ion from the cytosol (Fedrizzi and Carafoli, 2011). The increase of Ca^{2+} levels, deriving from the entry in the cytosol from the extracellular space or intracellular stores, generates Ca^{2+}-mediated signals linked to numerous processes. Thus, Ca^{2+} concentration and movements must be kept under careful control, so as to allow cells to function correctly. Were this control to fail, the cell would then be in serious danger because uncontrolled Ca^{2+} levels trigger vicious processes, including the cell demise (Carafoli, 2005).

In neurons, Ca^{2+}-mediated signals regulate also synaptic plasticity, neurite outgrowth and synaptogenesis (Mattson, 2007). Several reports have demonstrated that dysregulation of Ca^{2+} homeostasis is one of early events leading to neurodegeneration in disorders such as Alzheimer's, Huntington's and Parkinson's disease (Bezprozvanny, 2009). With respect to PrP^{C} pathophysiology, electrophysiologic studies, or use of chemical Ca^{2+} indicators, have highlighted that alterations of Ca^{2+} homeostasis occur in animal and cell models of prion infection, leading to impairment of Ca^{2+}-dependent neuronal excitability, long-term potentiation (LTP) and synaptic plasticity (reviewed in Peggion *et al.*, 2011). Importantly, similar disturbances have been reported in PrP-KO models. For example, electrophysiologic studies on CA1 hippocampal slices reported that PrP-KO neurons exhibited a significantly weakened LTP and reduced slow after hyperpolarization (AHP) than in WT neurons (Mallucci *et al.*, 2002; Powell *et al.*, 2008). It is good to remind that AHP and LTP are processes closely related to Ca^{2+} homeostasis. Indeed, AHP is mediated by Ca^{2+}-activated K^{+} channels whose activation causes membrane depolarization (Sah and Davies, 2000), while LTP, which involves Ca^{2+}-mediated glutamate receptors such as N-

methyl-D-aspartic acid (NMDAR)-, and α-amino-3-hydroxy-5-methyl-4-isoxazolepropionic acid (AMPAR)-, receptors (Lynch, 2004), works together with long-term depression (LTD) in regulating synaptic plasticity (essential for learning and memory).

More recently, Zamponi and coworkers have demonstrated a physical and functional interaction between PrP^C and the NMDAR (Khosravani *et al.*, 2008), whereby PrP^C would exert a neuroprotective role by selectively inhibiting a specific NMDAR subunit (NR2D). Accordingly, PrP-KO hippocampal neurons display increased excitability and enhanced glutamate excitotoxicity that can be reversed by blocking NMDAR activity. Other groups have demonstrated that PrP^C can associate also with, and modulate, other glutamate receptors, as kainite-sensitive receptors (GluR6/7), and group I metabotropic glutamate receptors (mGluR1 and mGluR5) following the binding of PrP^C to laminin γ1 chain (Ln- γ1) (Beraldo *et al.*, 2011; Carulla *et al.*, 2011). Specifically, in the case of GluR6/7, it has been proposed that PrP^C inhibits the interaction of GluR6/7 with the postsynaptic density 95 protein (PSD-95), thus protecting neurons from excitotoxicity and cell death (Carulla *et al.*, 2011). Instead, Beraldo *et al.* (2011) demonstrated that PrP^C bound to Ln- γ1 activates mGluR1 and mGluR5, and that the consequent Ca^{2+} release from the ER promotes the protein kinase C (PKC)-dependent activation of ERK1/2 that mediates neuritogenesis.

Use of aequorin isoforms, Ca^{2+}-sensitive photoprobes genetically targeted to specific cellular domains, has allowed our laboratory to provide more explicit insights into the involvement of PrP^C in the control of local (PM, cytosol, ER, mitochondria) Ca^{2+} homeostasis in model cells or primary cultured cerebellar granule neurons (CGNs) expressing, or not, PrP^C (Brini *et al.*, 2005; Lazzari *et al.*, 2011). By this approach, it was found that PrP-KO CGNs display a dramatic increase of store-operated Ca^{2+} entry (SOCE) and reduced steady-state ER Ca^{2+} levels with respect to WT neurons (Lazzari *et al.*, 2011), and that these effects could be due – at least in part – to the significantly decreased expression of the plasma membrane (PMCA)-, and sarco-ER (SERCA)-Ca^{2+}- ATPases in neurons lacking PrP^C.

1.5 PrP^C AND ALZHEIMER'S DISEASE

Alzheimer's disease (AD), described for the first time by Alois Alzheimer in 1907 (Alzheimer, 1907), is the most common cause of dementia in adults. AD is a multifactorial disease that has a genetic or sporadic nature. Although many therapeutics are now available to slow the neurodegenerative progression, as yet there is no efficient way to halt or prevent AD (Citron, 2010).

AD is characterized by the deposition inside neurons of neurofibrillary tangles (NFTs) composed of hyperphosporylated tau protein (a microtubule-associated protein), and of plaques, or amyloids, in the extracellular space (Katzman, 1986). The major constituents of plaques are the amyloid-β (Aβ) peptides (Glenner and Wong, 1984), which derive from the proteolytic cleavage of the transmembrane amyloid precursor protein (APP) by the activity of β- and γ-secretases. Initially, according to the *amyloid cascade hypothesis* (ACH) (Hardy and Higgins, 1992), tangles and plaques have been considered the primary cause of the pathogenesis of AD, whereby monomers of Aβ peptides would aggregate in dimers, trimers and higher order oligomers, ultimately forming the insoluble fibrils and plaques. Soon after, however, their correlation with disease onset and severity (Rushworth and Hooper, 2010) made it clear that soluble Aβ oligomers were the major neurotoxic species in AD. Aβ peptides can be composed by 36 to 43 amino acids; yet it is the Aβ1-42 peptide the prime suspect in AD pathogenesis, given its elevated levels in AD brains and the remarkable ability to aggregate in oligomers (Karran *et al.*, 2011).

To explain the relationship between Aβ toxicity and neurodegeneration, the *Ca^{2+} hypothesis of AD* has been proposed (Khachaturian, 1994), in light of data showing that Aβ oligomers disrupt neuronal Ca^{2+} homeostasis causing, in particular, a cytosolic Ca^{2+} overload by enhancing its entry from the extracellular space, and release from internal stores. This could well explain some AD-related processes such as excitotoxicity, impairment of LTP and LTD and neuronal apoptosis (Demuro *et al.*, 2010; Walsh *et al.*, 2002).

Ca^{2+} (dys)homeostasis is thus a trait common between AD and prion disease, but other aspects link the two disorders. For example, the Aβ deposits observed in some CJD cases (Muramoto *et al.*, 1992), the presence of PrP^C in plaques of a subset of AD brains (Voigtländer *et al.*, 2001), or the Met/Val 129 polymorphism of PRPN that is considered a possible risk factor for early onset-AD (Dermaut *et al.*, 2003). But the most recent and intriguing connection between PrP^C and AD is the proposition that PrP^C acts as a high-affinity receptor for Aβ oligomers and mediates their neurotoxic effects (Laurén *et al.*, 2009). After the first report, others have confirmed that Aβ1−42 oligomers indeed bind with high affinity the PrP^C central region (Balducci *et al.*, 2010; Calella *et al.*, 2010), but the notion that PrP^C is required for the Aβ oligomer-mediated cognitive impairment and cell death has been questioned. Indeed, a dispute on this issue is still ongoing, with reports favoring (Alier *et al.*, 2011; Barry *et al.*, 2011; Bate and Williams, 2011; Chen *et al.*, 2010; Chung *et al.*, 2010; Freir *et al.*, 2011; Gimbel *et al.*, 2010; Kudo *et al.*, 2012; Resenberger *et al.*, 2011; Um *et al.*, 2012; You *et al.*, 2012; Zou *et al.*, 2011) or denying (Cissé *et al.*, 2011; Kessels

et al., 2010) that PrP^C mediates Aβ-induced synaptic damage and neuronal demise. As for the mechanisms through which this may occur, however, it has been proposed that Aβ-PrP^C docking could cause LTP impairment through the activation on Fyn, a kinase member of the *Src* family of tyrosine kinases (SFK), which in turn would phosphorylate the NMDAR subunit NR2B, thus modifying NMDAR activity and promoting perturbations of Ca^{2+} homeostasis (Um *et al.*, 2012). A possible explanation for the discrepant results on the functional effects of Aβ -PrP^C interaction could reside in the use of different Aβ preparations, animals, tissues, AD models and type of behavioral tests.

Another dispute in the context of PrP^C-AD cross-talk was born on the possibility that PrP^C modulates Aβ production. On the one hand, Hooper and colleagues reported that the levels of Aβ peptides were higher in PrP-KO mice compared to control animals, and provided evidence that PrP^C down-regulates the production of Aβ in the brain through inhibition of β-secretase (Parkin *et al.*, 2007). On the other hand, other groups reported that the deletion of PrP^C failed to alter Aβ levels in transgenic mice expressing human APP with the Swedish familial mutations (APP_{Swe}) (Calella *et al.*, 2010; Gimbel *et al.*, 2010). This conundrum was eventually resolved when it was found that PrP^C interacts with, and retains, the immature form of β-secretase in the secretory pathway, thus reducing the amount of the protease at the cell surface and in endosomes. Of consequence, PrP^C has an inhibitory effect on the amyloidogenic processing of APP_{WT}, which is cleaved by β-secretase in endosomes, while exerting the opposite effect on APP_{Swe}, which is processed in the secretory pathway (Griffiths *et al.*, 2011). Thus, PrP^C differentially affects the metabolism of APP_{WT} and APP_{Swe}, suggesting that it may play a key protective role against sporadic AD.

In conclusion, the hypothesis that PrP^C is intimately linked to AD is plausible, in particular with respect to the production of, and binding to, Aβ peptides. However, the capacity to influence Aβ neurotoxic effects is more difficult to decode, not only for the ability of Aβ peptides to bind to other proteins and cell membranes, but also for the pleiotropic nature of PrP^C.

2. MATERIALS AND METHODS

2.1 ANIMALS

The animals used in this study were kindly provided by the MRC Prion Unit (London, UK), and belonged to the following congenic mouse lines (Mallucci *et al.*, 2002) bearing an almost pure FVB genotype:

- PrP-KO mice (line F10)
- transgenic mice (line Tg46) in which PrP^{C} expression was rescued at physiologic levels over the F10 PrP-KO genetic background.

In particular, the F10 PrP-KO line was generated by crossing for 10 generations $Prnp^{0/0}$ mice of the Zurich-I line (having a mixed Sv129/C57B genetic background, Büeler *et al.*, 1992) with WT FVB mice, after which $PrP^{+/-}$ mice were crossed with each other to obtain a PrP-KO progeny with an almost pure (>99%) FVB genotype. To rule out the possibility that any observed difference in our experiments could be due to the (<1%) background genetic difference between PrP-KO and WT FVB mice, we used as controls the Tg46 mouse line, given that this line has the same genetic background of F10 mice, except for the transgene containing the murine PrP coding region.

It is important to note that some of the PrP-KO phenotypes here described, which were evident at the beginning of the project, progressively disappeared over time. We reasoned that this could have been caused by a progressive genetic drift, due to the continuous inbreeding to which homozygous F10 mice were subjected. Thus, we decided to establish a new PrP-KO mouse colony starting from other F10 mice provided by the London MRC Prion Unit. Months were needed to re-establish a sufficiently expanded colony to perform experiments regularly. This substantially delayed the progression of the project. Of course, data obtained from mice suspected to underwent the hypothesized genetic drift were excluded by every kind of analysis presented here.

All aspects of animal care and experimentation have been performed in compliance with European and Italian (D.L. 116/92) laws concerning the care and use of laboratory animals. The Institution in which the work was carried out has been acknowledged by the Italian Ministry of Health, and by the Ethical Committee of the University of Padova, for the use of mice for experimental purposes.

2.2 PRIMARY CULTURES OF CEREBELLAR GRANULE NEURONS

Cerebellar granule neurons were obtained from 7 day-old mice and each CGN primary culture was prepared by combining cerebella derived from four to six littermates, as described in Levi *et al.* (1984). Animals were killed by decapitation, and the cerebellum was quickly removed and placed in ice-cold isolation buffer (IB) [124 mM NaCl, 5.4 mM KCl, 1 mM NaH_2PO_4, 0.5 mM $MgSO_4$, 3.6 mM dextrose, 0.3% (w/v) bovine serum albumin (BSA), 25 mM HEPES/KOH (pH 7.4)]. After carefully removing meningeal layers and blood vessels, the cerebellar tissue was gently minced and dissociated in 5 ml of IB added with trypsin (0.8 mg/ml) (12 min, 37°C). Trypsin activity was stopped by adding an equal volume of IB supplemented with deoxy-ribonuclease I (0.012 mg/ml) (Roche Corporation), a trypsin inhibitor (0.08 mg/ml) (Sigma), and 0.25 mM $MgSO_4$. After centrifugation (180 g, 5 min), the pellet was gently resuspended in IB (5 ml) supplemented with deoxyribonuclease I (0.08 mg/ml), the trypsin inhibitor (0.52 mg/ml), and 1.25 mM $MgSO_4$. After sedimenting the cell debris, the dissociated CGN-containing supernatant was added with an equal volume of IB containing 1.2 mM $MgSO_4$ and 1.4 mM $CaCl_2$, and centrifuged (180 g, 5 min). Finally, the pellet was gently resuspended in culture medium (Minimum Essential Medium Eagle (Sigma)), supplemented with 10% heat-inactivated foetal calf serum (Euroclone), 2 mM L-glutamine (Gibco), 0.1 mg/ml gentamycin (Gibco), and KCl (25.4 mM final K^+ concentration).

CGN were seeded at a density of $9 \cdot 10^5$ cells (onto poly-L-lysine-coated 13- mm coverslips) for immunocytochemistry and luminometer assays, or at a density of $3 \cdot 10^6$ cells (onto 35-mm poly-L-lysine-coated plates) for biochemical assays, and cultured in a humidified incubator (37°C, 5% CO_2 atmosphere). 48 h after plating, cytosine arabinoside (AraC, final concentration 0.04 mM, Sigma) was added to the culture to inhibit the proliferation of non-neuronal cells. CGN were always used after a total of 96 h in culture.

2.3 IMMUNOCYTOCHEMICAL ANALYSIS

Before experiments, the presence of astrocytes (the major non-neuronal contaminant of CGN cultures) was routinely checked following the immunocytochemical staining of an astrocytic marker (i.e., the glial fibrillary acidic protein, GFAP). To this purpose, 96 h-cultured CGN were rinsed twice with phosphate-buffered saline (PBS), fixed (30 min, 4°C) with paraformaldehyde [2% (w/v) in PBS], rinsed again, permeabilised (5 min, 4°C) with Triton-X100 [0.1% (w/v) in PBS], and treated with 50 mM NH_4Cl to quench cell auto-fluorescence. Cells were then incubated (1 h, 25°C) with anti-GFAP rabbit polyclonal antibody (pAb) (Dako), diluted (1 : 500) in PBS with BSA

0.5% (w/v). After extensive washings with PBS, cells were treated (1 h, 25°C) with FITC conjugated anti-rabbit IgG secondary antibody (Santa Cruz Biotechnology) [1 : 500 in PBS with BSA 0.5% (w/v)]. Finally, CGN were counter-stained with Hoechst 33258 (Molecular Probes, Invitrogen) (1 μg/ml in PBS) to visualize nuclei, and mounted with glycerol [30% (v/v) in PBS] onto glass slides for observation with an inverted fluorescence microscope (Axiovert 100, Zeiss), equipped with a computer assisted CCD camera (AxioCam, Zeiss). These assays indicated that contamination of 96 h-old CGN cultures by GFAP-positive cells was always below 3%.

2.4 CONSTRUCTION OF LENTIVIRAL VECTORS FOR AEQUORINS, AND CELL INFECTION

We have monitored fluctuations of Ca^{2+} concentrations [Ca^{2+}] in the cytosolic domains proximal to the PM ([Ca^{2+}]$_{pm}$), in the cytoplasm ([Ca^{2+}]$_{cyt}$), in the lumen of the endoplasmic reticulum (ER) ([Ca^{2+}]$_{er}$), or in the mitochondrial matrix ([Ca^{2+}]$_{mit}$). To this end, we have used a lentiviral expression system that transduces into CGN the chimeric constructs encoding aequorin (AEQ) linked to the influenza virus hemagglutinin (HA) epitope tag, and to defined targeting signals that determined the specific localization of the Ca^{2+} probe inside the cell. In particular, AEQ was N-terminally linked to the synaptic-associated protein 25 (SNAP-25), to the constant region (CH1 domain) of the Igγ2b heavy chain, or to the subunit VIII of human cytochrome c oxidase (COX8), which target the probe to PM subdomains (pmAEQ, Marsault *et al.*, 1997), the ER lumen (erAEQ, Montero *et al.*, 1995) and the mitochondrial matrix (mtAEQ, Rizzuto *et al.*, 1992), respectively. For cytosolic AEQ (cytAEQ, Brini *et al.*, 1995), no further modification was introduced in HA1-tagged AEQ construct.

The third generation packaging system used for this study includes 2 packaging plasmids (pMDLg/pRRE and pRSV-Rev), an envelope plasmid (pMD2.VSVG), and a transfer plasmid (pLV) in which the cDNA encoding one of the different AEQ chimeric constructs has been cloned. Lentiviral particles obtained with this system can infect both replicating and non-replicating cells (for example neuronal cells), and integrate their genetic material into the host cell allowing for stable, long-term expression of the transgene. They were produced as described in Follenzi and Naldini (2002). Briefly, HEK293T packaging cells ($15*10^6$ cells in 150 mm culture plates), cultured in Dulbecco's modified Eagle's medium (Sigma) supplemented with 10% foetal calf serum, 2 mM L-glutamine, 40 μg/ml penicillin/streptomycin (Euroclone), were co-transfected (24 h after plating) with pMDLg/pRRE, pMD2.VSVG, pRSV-Rev plasmids and the desired pLV-AEQ construct, by means of the calcium-phosphate transfection method. After 16 h, the transfection medium was replaced with fresh culture medium, and cells were grown for 72 h, after which the culture

medium was collected. Viral particles were harvested by ultracentrifugation (50 000 g, 2 h), resuspended in 0.2 ml of phosphate buffered saline (PBS), and stored at -80°C until use.

CGN were treated with lentiviral particles (diluted in culture medium) 24 h after plating, and, after additional 24 h, added with an equal volume of culture medium supplemented with 0.08 mM AraC (see above). Vector production and gene delivery were performed in a biosafety level-2 environment.

2.5 AEQ-BASED Ca^{2+} MEASUREMENTS

AEQ, originally isolated from the luminescent jellyfish *Aequorea Victoria*, is a 189 amino acid protein containing three high-affinity Ca^{2+}-binding sites (EF-hand type). The holo-protein is covalently linked to a hydrophobic prosthetic group, coelenterazine. Upon Ca^{2+} binding AEQ undergoes a conformational change that triggers the oxidation of the coelenterazione to coelenteramide, resulting in the emission of light (λ_{max} = 469 nm).

In our experiments, the chimeric apo-AEQ expressed by infected CGN was reconstituted into the active photo-protein form by adding coelenterazine to an appropriate incubation medium just before Ca^{2+} measurements. Light emission by holo-AEQ molecules then allowed the with-time monitoring of the Ca^{2+} concentration in the cell compartment/organelle to which the photo-protein was targeted.

AEQ-based Ca^{2+} measurements were performed by means of a computer-assisted luminometer equipped with a perfusion system, always using 96 h-cultured CGN. Depending on the type of the measurement, neurons were stimulated as described below.

All experiments ended by lysing cells with digitonin (100 μM, Sigma) in a hypotonic Ca^{2+}-rich solution (10 mM $CaCl_2$ in H_2O), to discharge the remaining aequorin pool. The light signal was digitalized and stored for subsequent analyses. Luminescence data were calibrated off-line into $[Ca^{2+}]$ values, using a computer algorithm based on the Ca^{2+} response curve of AEQ (Brini *et al.* 1995).

AEQ is well suited for measuring $[Ca^{2+}]$ between 0.5 and 10 μM. This optimal range, however, is frequently lower than the $[Ca^{2+}]$ variations occurring in some cell compartments. For this reason, it was necessary to reduce the Ca^{2+} affinity of the photoprotein (by ~50-fold) by the Asp119Ala mutation in the Ca^{2+} binding sites (Kendall *et al.*, 1992) (i.e. for the pmAEQ, mtAEQ and erAEQ), and to use a modified coelenterazine, *coelenterazine n* (in the case of erAEQ). These modifications allow measuring $[Ca^{2+}]$ higher than 100 μM.

For measuring Ca^{2+} movements elicited by SOCE (store operated Ca^{2+} entry, a mechanism of Ca^{2+} influx stimulated by depletion of intracellular Ca^{2+} stores, see chapter 3.3.1), in the cytosolic domains beneath the PM, the cytosol, and the mitochondria, CGN were incubated (1 h, 37°C, 5% CO_2 atmosphere) in modified Krebs-Ringer buffer [KRB, 125 mM NaCl, 5 mM KCl, 1 mM Na_3PO_4, 1 mM $MgSO_4$, 5.5 mM glucose, 20 mM HEPES (pH 7.4)] supplemented with EGTA (100 μM) (to deplete intracellular Ca^{2+} stores), and the prosthetic group coelenterazine (5 μM, Fluka) (to reconstitute functional pmAEQ, cytAEQ or mtAEQ). After transferring the cell-containing coverslip to the thermostatted chamber of the luminometer, experiments started by perfusing cells with KRB, first containing EGTA (100 μM), then $CaCl_2$ (1 mM), which resulted in transients $[Ca^{2+}]$ rises in all monitored cell domains. Then, after about 700 s, during which $[Ca^{2+}]$ returned to the basal level in the different cell domains, cells were perfused for 30 seconds with Mg^{2+}-free KRB containing $CaCl_2$ (1 mM), and then with the same buffer added with glutamate (100 μM) (Sigma) and glycine (10 μM) (Sigma). This protocol elicited a second Ca^{2+} transient due to Ca^{2+} entry from the extra-cellular space through ionotropic glutamate receptors, and release of the ion from the ER through inositol 1,4,5-triphosphate (IP_3)-sensitive channels activated via metabotropic glutamate receptors at the PM. In other experiments, glutamate was replaced by NMDA (50 μM), to stimulate ionotropic NMDA receptors exclusively.

A different protocol was used when measuring $[Ca^{2+}]_{er}$ by means of erAEQ. In this case, CGN were washed three times with KRB supplemented with 1 mM EGTA, left 10 min at 37°C (5% CO_2 atmosphere), and then incubated (1 h, 4°C) in KRB supplemented with 5 μM ionomycin (Sigma), 500 μM EGTA and 5 μM coelenterazine n (Tebu-bio Italy). After transferring the coverslip to the luminometer chamber, experiments started by perfusing cells with KRB containing (in sequence): 500 μM EGTA (2 min); 2% BSA and 1 mM EGTA (3 min); 500 μM EGTA (2 min); 1 mM $CaCl_2$. This protocol provided a means of replenishing intracellular stores, and was followed by perfusion with KRB containing EGTA (100 μM) and glutamate (100 μM) to provoke Ca^{2+} release from the ER through IP_3-sensitive channels stimulated by metabotropic glutamatergic receptors.

2.6 Aβ1-42 PEPTIDE PREPARATION AND TREATMENT

Aβ1-42 oligomers were prepared according to the following procedure. Chemically synthetized and lyophilized Aβ1-42 peptides (kindly provided by Dr. A.F. Hill - Univ. of Melbourne) were dissolved in 1 mg/ml of 1,1,1,3,3,3-hexafluoro-2-propanol (HFIP) and incubated (1 h, room temperature (RT)) to remove pre-existing aggregates. The suspension was then divided into aliquots (each consisting of about 50 μg of peptide), HFIP was removed by evaporation, and

aliquots were stored at -80°C. Just before use, each peptide aliquot was dissolved in 20 mM NaOH (50 µl), sonicated (15 min on ice) in a bath sonicator, and diluited in PBS to a final volume of 250 µl. The suspension was then centrifuged (14,000 g, 5 min) to pellet aggregates, and Aβ1-42 concentration was measured by absorbance spectrophotometry (λ = 214 nm). Finally, Aβ1-42 peptides were incubated (1 h, 37°C) to obtain oligomers, and then administered to CGN at a final concentration of 5 µM of monomer equivalent. Incubation of CGN with Aβ1-42 oligomers was carried out during the AEQ reconstitution step (see above) in KRB supplemented with EGTA and coelenterazine (1 h, 37°C, 5% CO_2 atmosphere).

2.7 CHARACTERIZATION OF Aβ1-42 PEPTIDE

For each used aliquot of the Aβ1-42 peptide, we performed qualitative analyses by Western blotting to characterize the oligomerization state of each preparation. To this purpose, small peptide samples (~300 ng) were collected both before and after the oligomerization process. Samples were immediately diluted in a sample buffer containing 12% sodium dodecyl-sulphate (SDS) (w/v), 6% mercaptoethanol (v/v), 30% glycerol (w/v), 0.05% Coomassie blue, 150 mM Tris/HCl (pH 7.0), and were separated using a urea (6M)-containing tricine gel (16% (w/v) acrylamide) that offers a high resolution capacity in the small proteins and peptides range (Schägger, 2006).

Proteins were then electro-blotted onto polyvinylidene fluoride (PVDF) membranes of 0.22 µm pore size (Millipore). Membranes were incubated (1 h, RT) with a blocking solution containing non-fat dry milk (5% (w/v), Bio-Rad) diluted in Tris-buffered saline added with 0.02% (w/v) Tween-20 (TBS-T 0.02%). Then, membranes were incubated over-night (4 °C) with anti-Aβ mouse monoclonal antibody (mAb) 6E10 (Covance) diluited (1:1000) in the blocking solution. After three 10 min-washes with TBS-T 0.02%, membranes were incubated (1 h, RT) with a horseradish peroxidase-conjugated anti-mouse IgG secondary antibody (Santa Cruz Biotechnology) (1 : 3000 in the blocking solution). Immunoreactive bands were visualized and digitalized by means of a digital Kodak Image Station, using an enhanced chemiluminescence reagent kit (Millipore). For densitometric analysis, band intensities were evaluated by the Kodak 1D image analysis software.

2.8 WESTERN BLOT ANALYSES PrP^C AND SYNAPTOPHYSIN EXPRESSION, AND FOR $p59^{Fyn}$ AND Erk1/2 ACTIVATION

For Western blot assays, CGN were homogenized in either Laemmli sample buffer (10% glycerol (w/v), 2% (w/v) SDS, 62.5 mM Tris/HCl (pH 6.8), protease inhibitor cocktail (Roche)) for PrP^C and

synaptophysin expression, or a buffer containing 10% glycerol (w/v), 2% (w/v) SDS, 62.5 mM Tris/HCl (pH 6.8), 1.8 M Urea, 5 mM $NaVO_4$, protease inhibitor and phosphatase inhibitor cocktails (Roche), for analyzing of $p59^{Fyn}$ and ERK 1/2 activation, and boiled (5 min). The total protein content was determined by the Lowry method (Total Protein Kit, Micro Lowry, Peterson's Modification, Sigma), using BSA as standard. Dithiothreitol (50 mM) and bromophenol-blue (0.004% (w/v)) were added to samples just before gel loading. SDS-PAGE was carried out using 10% acrylamide, and 20 μg of proteins loaded in each lane. Proteins were then electro-blotted onto nitrocellulose membranes (Bio-Rad Laboratories, Hercules, CA, USA), which were stained with Ponceau red (Ponceau S, Sigma) to verify equal loading and transfer. Membranes were incubated (1 h, RT) with a blocking solution that, depending on the used antibody, contained TBS added with 0.1% (w/v) Tween-20 (TBS-T) and 5% (w/v) non-fat dry milk, for synaptophysin; TBS-T added with 3% (w/v) BSA, for phospho-Src (pSrc), $p59^{Fyn}$, phospho-Erk1/2 (pErk1/2) and total Erk1/2; or PBS added with 0.1% (w/v) Tween-20 (PBS-T) and 3% (w/v) BSA, for PrP^C and β-actin. Membranes were then incubated with the desired primary antibody (1 h, RT) diluted (see below) in the corresponding blocking solution. After three 10 min-washes with TBS-T (or PBS-T), membranes were incubated (1 h, RT) with a horseradish peroxidase-conjugated anti-mouse or anti-rabbit IgG secondary antibody (Santa Cruz Biotechnology) (1:3000 in the blocking solution), depending on the used primary antibody (see below). Immunoreactive bands were visualized and digitalized by means of a digital Kodak Image Station, using an enhanced chemiluminescence reagent kit (Millipore). For densitometric analysis, band intensities were evaluated by the Kodak 1D image analysis software, and normalized to the optical density of the corresponding lane stained with Ponceau red. For assessing the phosphorylation (activation) state of $p59^{Fyn}$ and Erk1/2, samples were always run in duplicate, and then probed in parallel with antibodies recognizing either the phosphorylated (p) and non-phosphorylated (total) forms of the target protein. The immunosignal intensity of pSrc and pErk1/2 was the normalized to those of total $p59^{Fyn}$ and total Erk1/2, respectively.

Antibodies

For immunoblotting, the following antibodies were used (dilutions in parenthesis): anti-PrP mouse monoclonal (m) antibody (Ab) 8H4 (1 : 6000, a kind gift of Dr. M. S. Sy, Case Western University, Cleveland, OH); anti-β-actin mouse mAb (1 : 4000, Sigma, cat. N. A5441); anti-synaptophysin rabbit polyclonal (p) Ab (1 : 2000, ProteinTech Group, cat. N. 17785-1-P); anti-$p59^{Fyn}$ rabbit pAb (1:1000, Cell Signalling Technology, cat. N. 4023); anti-pSrc rabbit pAb (recognizing the activatory phospho-site in all SFKs, which corresponds to pY416 in p59Fyn) (1:1000, Cell Signalling Technology, cat. N. 2101); anti- pErk1/2 mouse mAb (1:1500, Cell

Signalling Technology, cat. N. 9106S); anti-total Erk1/2 rabbit pAb (1:1500, Cell Signalling Technology, cat. N. 9102).

AIM OF THE WORK

Multiple and often contrasting experimental evidence, obtained by using cellular and animal models, has paradoxically thwarted the understanding of the physiological significance of PrP^C. Indeed, PrP^C has been implicated in a plethora of cellular processes, from copper metabolism to the defense mechanisms against oxidative and apoptotic challenges, to the promotion of cell adhesion and maturation (Linden *et al.*, 2008). In light of these multiple functions, a reasonable hypothesis is that the PrP^C acts as a scaffold protein in different cell surface complexes, and that specific downstream signaling pathways get activated depending on the type and state of the cell, the expression level of PrP^C, and the local availability of extracellular and/or intracellular signaling PrP partners (Peggion *et al.*, 2011). It is also possible to hypothesize that the common denominator of the various PrP^C roles is Ca^{2+}, the major and multifaceted intra-cellular messenger, able to control - just as it has been proposed for PrP^C - a large number of (patho)physiological processes ranging from cell survival to death.

The aim of this thesis was focused exactly on whether aspects of Ca^{2+} metabolism are governed by PrP^C. This aim was pursued using primary cultures of cerebellar granule neurons (CGN) derived from mice expressing (Tg46) or not (PrP-KO) PrP^C, and subjected to different Ca^{2+}-mobilizing stimuli. Use of Ca^{2+}-sensitive photo-proteins (aequorins) genetically targeted to different cell domains allowed us to monitor local fluxes, i.e., at the plasma membrane, the cytosol, the lumen of the endoplasmic reticulum and the mitochondrial matrix, and to relate these movements to the presence of PrP^C. In an attempt to rationalize our findings by a molecular point of view, we also analyzed important signaling pathways through which PrP^C could regulate Ca^{2+} homeostasis.

Adding further interest and complexity to the puzzling picture of PrP^C pathophysiology, recent findings have provided evidence that PrP^C acts as a high-affinity receptor for Aβ1-42 peptide oligomers (Laurén *et al.*, 2009; Balducci *et al.*, 2010; Calella *et al.*, 2010; Chen *et al.*, 2010; Freir *et al.*, 2011; Zou *et al.*, 2011), which are considered the prime responsible for AD pathogenesis. However, while some reports proposed that PrP^C-Aβ interactions are crucial to AD-related impairment of synaptic plasticity and memory formation (Laurén *et al.*, 2009; Gimbel *et al.*, 2010; Alier *et al.*, 2011; Barry *et al.*, 2011; Freir *et al.*, 2011; Um *et al.*, 2012; You *et al.*, 2012), others have argued against this possibility (Balducci *et al.*, 2010; Calella *et al.*, 2010; Kessels *et al.*, 2010; Cissé *et al.*, 2011). Based on the notion that neuronal Ca^{2+} homeostasis is intimately related to learning and memory, and given availability of the above suited protocols and cell

paradigms, the present thesis has also investigated if and how oligomeric Aβ peptides induced PrP^C-dependent alterations of Ca^{2+} movements.

3. RESULTS AND DISCUSSION

The study of the physiology of PrP^C – the major topic of the present Ph.D. thesis – was carried out in the cell model system represented by primary neuronal cultures, specifically cerebellar granule neurons (CGNs), obtained from mice expressing (Tg46), or not (PrP-KO), PrP^C. It is important to note that we have taken as true control the CGN those obtained from the transgenic Tg46 mice rather than from WT (FVB) mice, given that Tg46 animals express normal levels of PrP^C (Lazzari *et al.*, 2011) over the same genotype of the F10 PrP-KO mouse line (Mallucci *et al.*, 2002). In other words, the only aspect that discriminates Tg46 from PrP-KO neurons is the presence of the PrP gene.

The first part of the work was focused on the role of PrP^C in neuronal Ca^{2+} homeostasis. We pursued this goal by subjecting CGN (harboring or not PrP^C) to stimuli that trigger cell Ca^{2+} movements, and by monitoring the movements using the Ca^{2+}-sensitive AEQ probes. The second part of the thesis was instead devoted to understanding whether PrP^C is directly involved in $A\beta(1\text{-}42)$ oligomers-mediated impairment of Ca^{2+} homeostasis, which could sustain the current hypothesis that PrP^C acts as the receptor for $A\beta$-oligomers.

3.1 PURITY OF PRIMARY CGN CULTURES

By necessity, one of the first parameter of cultured CGN that we analyzed was the possible contamination by other cell types, specifically by astrocytes given their high replicative capacity. To this end, 96h-cultured CGN were routinely subjected to immunocytochemical assays using an antibody against the astrocytic marker, GFAP (Glial Fibrillary Acidic Protein). As shown in Fig.1, we found that the ratio between the number of astrocytes and the total number of cells labeled with the nuclear marker Hoechst, was on average less than 3%. This result allowed us to conclude that the (97%) degree of purity of the used CGN cultures was in accord with what reported in the literature (Carafoli *et al.*, 1999).

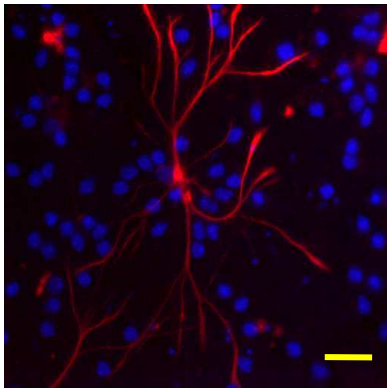

Figure 1. Immunocytochemical assay shows that CGN cultures were > 97% pure.
After 96 h in culture, CGN were fixed, permeabilised, and immunostained with an anti-GFAP pAb (red signal), and then counterstained with the nuclear marker Hoechst 33258 (blue signal). On average, the degree of contamination by astrocytes was less than 3%. Scale bar, 40 μm.

3.2 *In vitro* CGN MATURATION, AND DEVELOPMENTAL PrP^C EXPRESSION IN Tg46 CGN

The second control consisted in analyzing the expression levels of PrP^C during the *in vitro* neuronal differentiation process. As shown in Figure 3, Western blot analyses demonstrated that PrP^C expression progressively increased from 24 to 96 h in Tg46 CGN, and that, as expected, PrP^C was absent in PrP-KO neurons. This data indicates that suitable levels of PrP^C are present in Tg46 neurons when subjected to experimentation.

Another necessary control consisted in verifying if, at the culture time point at which Ca^{2+} measurements were performed, the PrP-KO CGN presented the same *in vitro* differentiation degree as their control counterpart. Growth of primary CGN in a medium supplemented with high concentrations of KCl (25.4 mM) is known to improve the long-term survival and purportedly mimics endogenous activity in developing cerebellum (Gallo *et al.*, 1987). To ascertain whether this *in vitro* condition determined a similar maturation of PrP-KO and Tg46 CGN, we followed by Western blot the with-time expression of synaptophysin, a synaptic vesicle membrane protein (Elferink and Scheller, 1993), at different time points after CGN plating. As shown in Figure 2, the progressive rise of synaptophysin expression from 24 to 96 h indicates the progressive synaptic maturation of both Tg46 and PrP-KO CGN. Importantly, given that at each time point no statistically significant difference was observed in the expression of synaptophysin in CGNs with different PrP genotype, we could conclude that the absence of PrP^C did not influence the *in vitro* maturation degree of neurons, in particular at 96 h of culture when neurons were used for AEQ-based experimentation and other tests.

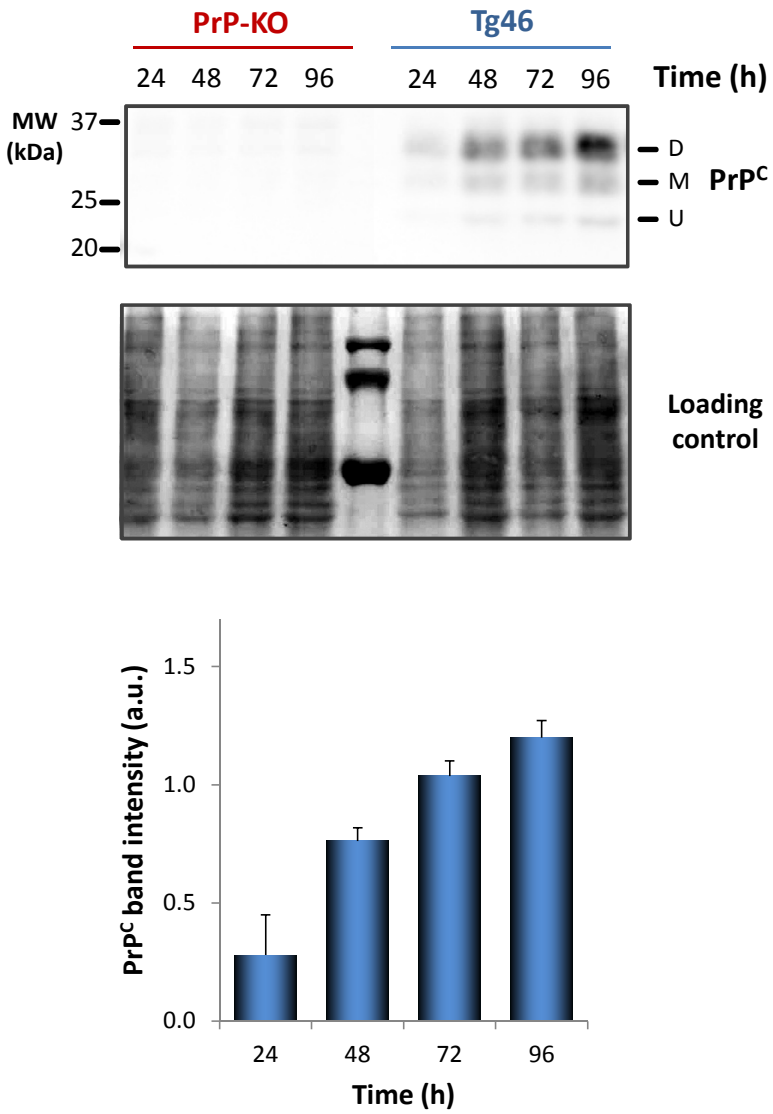

Figure 2. PrP^C expression progressively increases during the maturation of CGN obtained from Tg46 mice.

Tg46 and PrP-KO CGNs from 24 h to 96 h in culture were lysed and proteins (20 µg per lane) resolved by 10% SDS-PAGE under reducing conditions, electroblotted, and probed with an anti-PrP mAb 8H4. In the upper panel, a Western blot representative of 4 independent experiments is shown. To demonstrate equal protein loading and transfer, nitrocellulose membrane staining Ponceau red is also shown. Molecular mass standards are reported on the left. While in PrP-KO neurons no PrP-immunosignal is detectable, the expression level of all glycoforms of PrP^C, i.e., unglycosylated (U), mono-glycosylated (M) and di-glycosylated (D) (right arrows), progressively increases during the differentiation of Tg46 CGN. This latter finding is also clearly shown by the bar diagram of the lower panel, reporting the densitometric analysis of PrP immuno-reactive bands from Tg46 samples. Values are mean ± SEM, n =4.

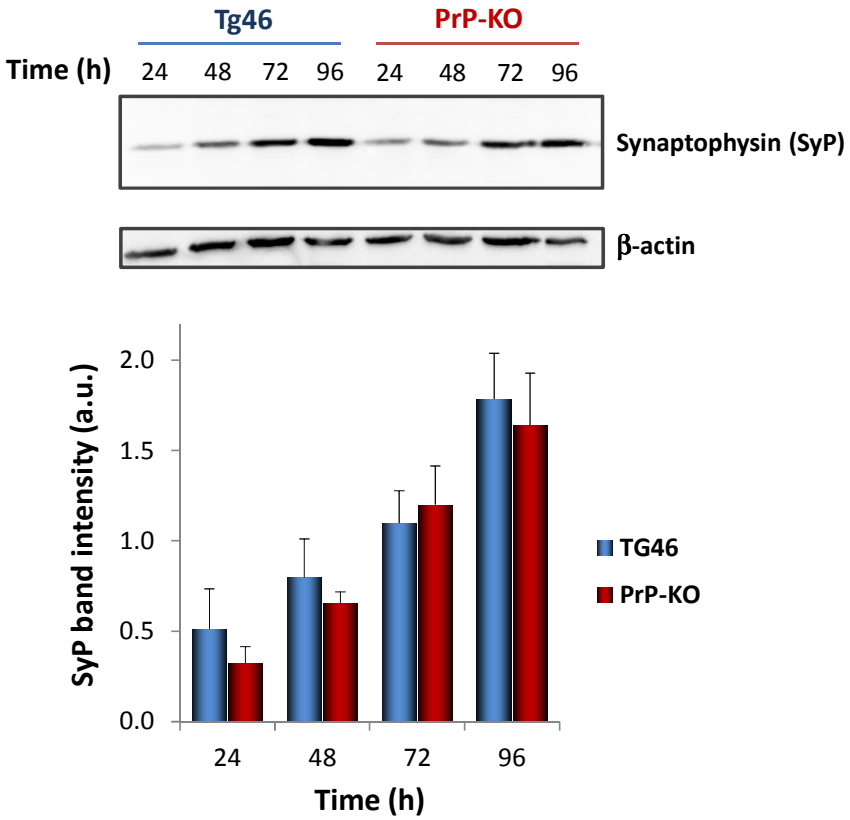

Figure 3. *In vitro* cultured CGNs progressively mature in PrP-independent manner.
Tg46 and PrP-KO CGNs at different times *in vitro* were assayed for SyP expression by Western blot with anti-synaptophysin (SyP) pAb, detecting a 38 kDa band. In the upper panel, a Western blot representative of 4 independent experiments for each genotype, is shown. To verify equal protein loading and transfer, the same blot was immunolabelled with an anti-β-actin mAb. In the lower panel, the densitometric analysis of synaptophysin expression in Tg46 (blue bars) and PrP-KO (red bars) CGNs is reported. It is evident that the expression of the synaptic marker progressively increases from 24 to 96 h in both CGN genotypes, and that no statistically significant difference exists between Tg46 and PrP-KO neurons for all time points. Values are mean ± SEM, n=4.
Other experimental details are as in the legend to Figure 2.

3.3 INVOLVEMENT OF PrP^C IN LOCAL Ca^{2+} MOVEMENTS INDUCED IN CGN BY DIFFERENT STIMULI

3.3.1 INVOLVEMENT OF PrP^C IN LOCAL Ca^{2+} MOVEMENTS INDUCED BY SOCE

Depletion of intracellular Ca^{2+} stores, primarily the ER, triggers the opening of Store-Operated Ca^{2+} Channels (SOCCs), and the consequent influx of Ca^{2+} from the extra-cellular space. This process, named Store-Operated Ca^{2+} Entry (SOCE) (or Capacitative Calcium Entry), serves to refill intracellular stores and to elaborating long-term Ca^{2+} signals (Parekh and Putney, 2005).

Little is known about the mechanisms of SOCCs activation, and the impact of this process in neuronal Ca^{2+} homeostasis. Two protein families, however, have been identified as essential

components in SOCE: STIM (for **S**tromal **I**nteraction **M**olecule) proteins, which are ER trans-membrane proteins with EF hand domains that project into the ER lumen and permit the protein to act as a sensor for luminal [Ca^{2+}]; Orai proteins, located to the PM and identified as the pore-forming subunits of SOCCs. It has been proposed that, upon depletion of ER Ca^{2+} stores, Ca^{2+} dissociates from the STIM EF-hand module, leading to oligomerization and redistribution of STIM molecules into discrete ER membrane clusters opposed to the PM. This would promote the physical interaction of STIM with Orai, the consequent recruitment of Orai into PM clusters, and the ultimate activation of SOCE (Cahalan, 2009; Varnai *et al.*, 2009).

Physiologically, SOCE is evoked by increased [IP_3], which binds to, and opens, IP_3 receptors at the ER membrane (Takemura *et al.*, 1989), or by other Ca^{2+}-releasing signals followed by Ca^{2+} release from the stores (Parekh and Putney, 2005). Experimentally, however, the most suited way to promote recordable SOCE relies on emptying ER Ca^{2+} stores by prolonged incubation of cells in the absence of Ca^{2+}. Thus, the first set of experiments here described started with 1h-incubation of CGN in KRB supplemented with the prosthetic group coelenterazine and EGTA (see Materials and Methods), serving to trigger both the reconstitution of functional holo-AEQ, and a substantial release of ER Ca^{2+} leading to SOCCs activation.

The resulting local Ca^{2+} transients in different cell domains were compared in Tg46 and PrP-KO CGN expressing the different AEQ chimerae (Fig. 4). In particular, Fig. 4A shows that the transient rise of $[Ca^{2+}]_{pm}$ had a significantly higher (~40%) peak value (30.40 ± 1.48 μM, PrP-KO CGN; 21.41 ± 0.56 μM, Tg46 CGN), and was more persistent, in PrP-KO CGN compared to Tg46 neurons. These results closely resemble when comparing PrP-KO with WT (FVB) CGN (Lazzari *et al.*, 2011), thus supporting the contention that Tg46 neurons are indeed suitable control model cells.

That plasma membrane domains of PrP-KO CGN accumulate more Ca^{2+} than control neurons was also reflected by the higher SOCE-evoked Ca^{2+} transients observed both in the cytosol (Fig. 4B, 1.26 ± 0.06 μM, PrP-KO CGN; 1.08 ± 0.05 μM, Tg46 CGN) and the mitochondrial matrix (Fig. 4C, 26.11 ± 0.93 μM, PrP-KO CGN; 21.84 ± 1.01 μM, Tg46 CGN). In light of all results shown in Fig. 4, one may thus conclude that it makes sense that the most remarkable difference between PrP-KO and Tg46 neurons regards [Ca^{2+}] variations occurring in sub-PM domains, i.e. in those domains in which the AEQ probe are likely to sense at best Ca^{2+} influx through activated SOCCs. Importantly, however, these findings convincingly demonstrate – for the first time – that PrP^C is somehow able to govern the entire neuronal SOCE-dependent neuronal Ca^{2+} homeostasis.

We also monitored ER Ca^{2+} refilling induced by SOCE. Given that ER accumulates large Ca^{2} amounts that would rapidly consume erAEQ impeding, therefore, reliable Ca^{2+} measurements, a specific protocol had to be applied (see Material and Methods). As shown in Fig. 5, SOCCs stimulation by this protocol allowed us to observe that both Tg46 and PrP-KO CGN recovered the luminal Ca^{2+} levels with similar kinetics that, however, led to a final steady-state $[Ca^{2+}]_{er}$ that was significantly lower (~20%) in PrP-KO CGN (211.44 ± 9.79 µM) than in PrP^{C}-expressing neurons (254.49 ± 17.44 µM).

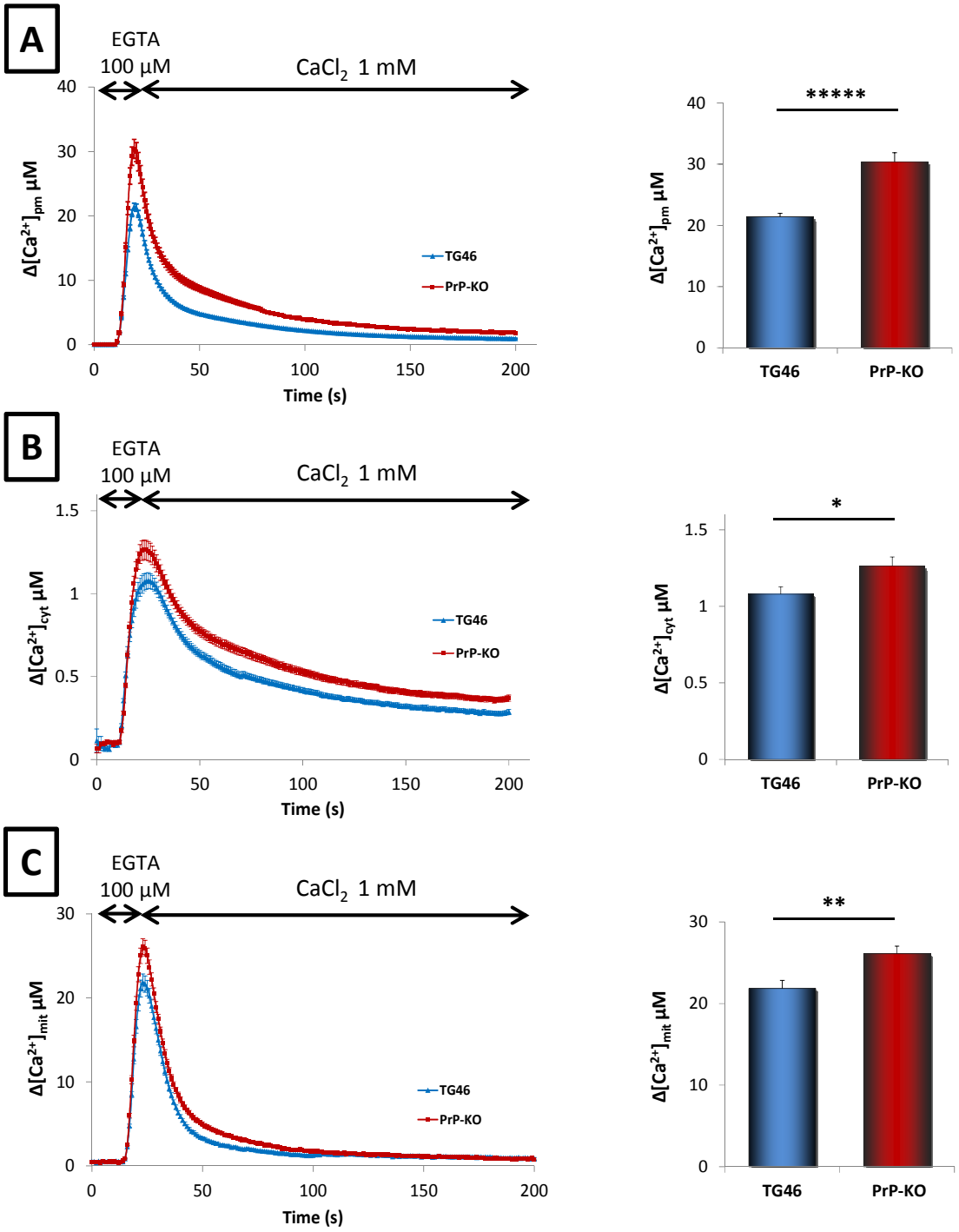

Figure 4. The transient increase of $[Ca^{2+}]_{pm}$, $[Ca^{2+}]_{cyt}$, and $[Ca^{2+}]_{mit}$ induced by SOCE is higher in PrP-KO CGN with respect to Tg46 neurons.

96 h after plating, Tg46 (TG46, blue) and PrP-KO (PrP-KO, red) CGN expressing pmAEQ (A), cytAEQ (B), or mtAEQ (C) were stimulated by SOCCs activation, following the depletion of intracellular Ca^{2+} store by incubation in EGTA (100 µM), and subsequent perfusion of cells with a $CaCl_2$ (1 mM)-containing buffer. Both the mean of the recorded traces (left panels), and the peak values reported in the bar diagrams (right panels) show that in all the AEQ-monitored cell compartments PrP-KO CGNs accumulate a higher $[Ca^{2+}]$ compared to PrP-expressing neurons. In addition, a slower rate of recovery to steady-state values of $[Ca^{2+}]_{pm}$ and $[Ca^{2+}]_{cyt}$ also pertains to PrP-KO CGNs with respect to Tg46 neurons. Values are mean ± SEM; n = 174 (Tg46) and 169 (PrP-KO) in (A), n = 41 (Tg46) and 57 (PrP-KO) in (B), n = 56 (Tg46) and 70 (PrP-KO) in (C), where n indicates the total number of traces used for the analysis (technical replicates). These traces derived from 20 (for both Tg46 and PrP-KO) independent CGN cultures (biological replicates) in (A), 10 (Tg46) or 12 (PrP-KO) biological replicates in (B), 10 (Tg46) or 13 (PrP-KO) biological replicates in (C). *****$p < 10^{-7}$; **$p < 0.01$; *$p < 0.05$ Student's t-test.

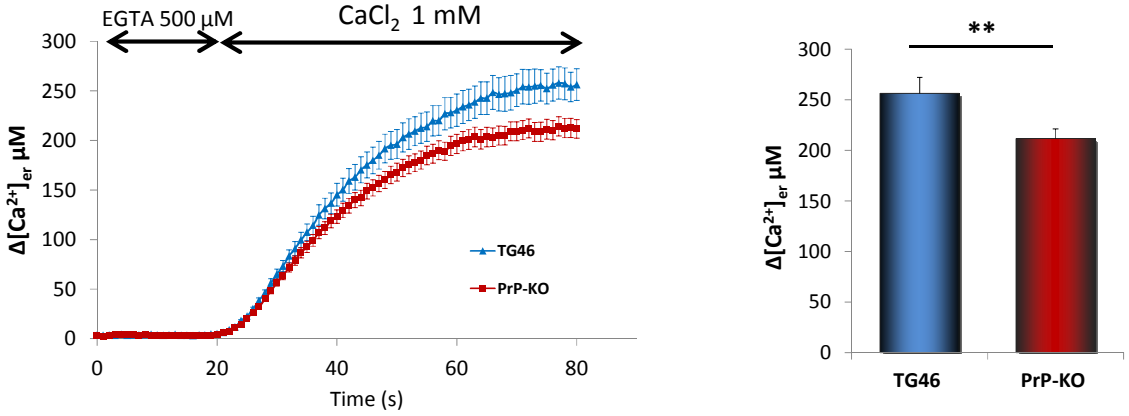

Figure 5. Steady-state Ca^{2+} levels in the lumen of the ER are significantly reduced in PrP-KO CGN.

erAEQ-expressing Tg46 (TG46, blue) and PrP-KO (PrP-KO, red) neurons were first depleted of stored Ca^{2+} by incubation in a Ca^{2+}-free buffer containing EGTA (500 µM) and the Ca^{2+} ionophore, ionomycin (5 µM), after which ER refilling was stimulated by perfusing cells with a $CaCl_2$ (1 mM)-supplemented buffer. Both the mean of the recorded traces (left panels) and the peak values reported in the bar diagrams (right panels) show that the steady-state level of $[Ca^{2+}]_{er}$ is significantly lower in PrP-KO CGN than in Tg46 neurons. Reported traces are mean ± SEM; n = 23 for both Tg46 and PrP-KO; biological replicates were 9 for each mouse strain. **p<0.01, Student's t-test.

3.3.2 INVOLVEMENT OF PrP^C IN LOCAL Ca^{2+} MOVEMENTS INDUCED BY STIMULATION OF ALL CELL GLUTAMATE RECEPTORS

After SOCCs-induced Ca^{2+} measurements were completed, CGN were carefully washed and then perfused with Mg^{2+}-free KRB containing $CaCl_2$ (1 mM), glutamate (100 µM) and glycine (10 µM). This protocol was intended to monitor Ca^{2+} transients due to activation of glutamate sensitive-receptors, i.e., both ionotropic (NMDAR, AMPAR and the kainate receptor) and metabotropic receptors (mGluR).

Glutamate is the major excitatory neurotransmitter in the brain and is involved in several neuronal functions, including cognition, memory and learning. Physiologically, the neurotransmitter binds to, and opens, AMPAR with the consequent entry of mono- and di-valent cations (Ca^{2+}, Na^{+} and K^{+}). This causes a partial depolarization of the cell potential that, by removing Mg^{2+} present in NMDARs, allows activation of NMDARs when the co-agonist glycine is also present (Traynelis *et al.*, 2010). Activity of all ionotropic receptors (including the kainate-sensitive receptors) thus allows a substantial entry into the cell of extracellular Ca^{2+}, which explains why, if present in abnormally high amounts, glutamate can be highly toxic to neurons (Nedergaard *et al.*, 2002). Instead, mGluRs are members of the G-protein-coupled receptor (GPCR) superfamily and are classified into three groups, group I (mGluRs 1 and 5), group II (mGluRs 2 and 3) and group III (mGluRs, 4, 6, 7, and 8). In particular, while G_q-coupled group I mGluRs activate phospholipase C, resulting in the generation of IP_3 and diacylglycerol that mobilize Ca^{2+} from ER and activate PKC, respectively, group II and III mGluRs are coupled predominantly to G_i proteins that ultimately inhibit adenylyl cyclase and the formation of cAMP (Niswender and Conn, 2010).

To best stimulate all receptors, including NMDAR, CGN were incubated with 100 μM glutamate and glycine in the absence of Mg^{2+}. Fig. 6 shows Ca^{2+} transients monitored by pmAEQ (6A), cytAEQ (6B) and mtAEQ (6C) in PrP-KO and Tg46 CGN. Clearly, in all domains Ca^{2+} fluxes were higher in PrP-KO neurons than in the control CGN – in plasma membrane domains the difference reached as much as 60% - although absolute [Ca^{2+}] variations were always smaller than those elicited by SOCE (peak values: in PM domains, 5.62 ± 0.18 μM, PrP-KO CGN and 3.56 ± 0.13 μM, Tg46 CGN; in cytosol, 2.37 ± 0.14 μM, PrP-KO CGN and 2.00 ± 0.07 μM, Tg46 CGN). A possible reason for this difference is that in the latter case the protocol probably maximizes ER-Ca^{2+} depletion and SOCCs stimulation.

Interestingly, also the peak value of $[Ca^{2+}]_{mit}$ observed in PrP-KO neurons (142.19 ± 9.72 μM) was much higher (50%) than in Tg46 neurons (91.36 ± 3.74 μM) (Fig. 6C). This result prompt us to verify whether PrP^{c} had a direct impact on mGluRs and/or the activated pathway, such as, for example, IP_3 receptors that facilitate Ca^{2+} entry into mitochondria via the close apposition of ER and mitochondrial membranes (Rizzuto *et al.*, 1993). To this end, we set out to follow Ca^{2+} release from ER stores using erAEQ and glutamate to stimulate preferentially mGluR, which was accomplished by adding EGTA in the perfusing medium but omitting glycine addition. Parenthetically, the presence of EGTA was also intended to maximally accelerate ER Ca^{2+} release. As shown in Fig. 7, we found that under these conditions the Ca^{2+} released by the ER of PrP-KO

CGN and Tg46 neurons was almost identical both in terms of kinetics and quantity. Thus, if these results clearly indicate that the activity of IP_3 receptors is not influenced by PrP^c, we still cannot definitively exclude that PrP^c influences the number of ER-mitochondrial junctions and/or the activity of the mitochondrial uniporter, the ultimate actor of mitochondrial Ca^{2+} accumulation.

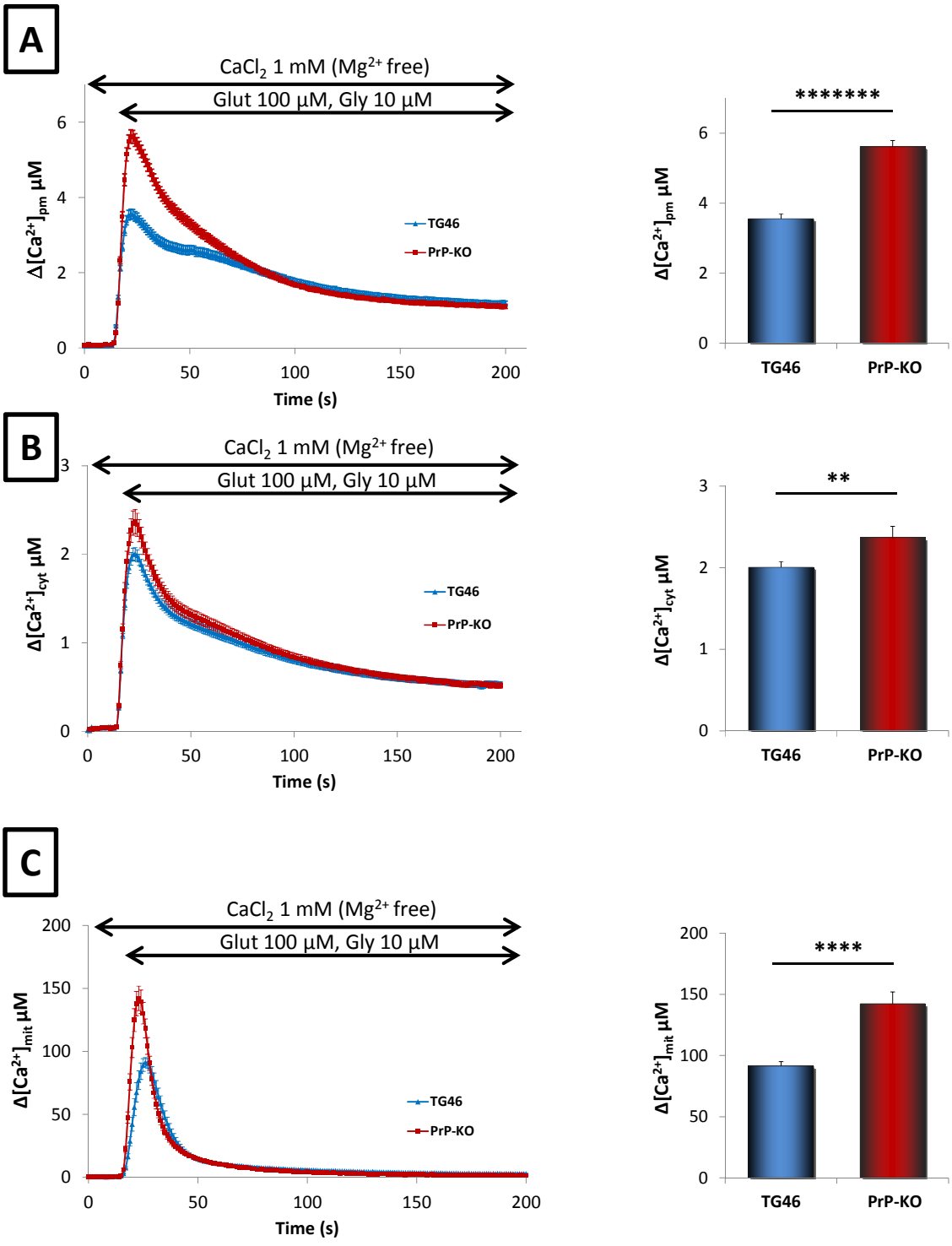

Figure 6. Activation of (ionotropic and metabotropic) glutamate receptors elicits $[Ca^{2+}]_{pm}$, $[Ca^{2+}]_{cyt}$, and $[Ca^{2+}]_{mit}$ transients that are significantly larger in PrP-KO CGNs than in Tg46 neurons.

Tg46 (blue) and PrP-KO (red) CGNs expressing pmAEQ (A), cytAEQ (B), or mtAEQ (C) were stimulated with glutamate (100 µM) and glycine (10 µM) in a Mg^{2+}-free, $CaCl_2$ (1 mM)-supplemented buffer. This protocol provokes the activation of both ionotropic and metabotropic glutamate receptors, and $[Ca^{2+}]$ transients in the different cell domains that were recorded by means of the targeted AEQ probes. Both the mean of the recorded traces (left panels), and the peak values reported in the bar diagrams (right panels) show that in all the AEQ-monitored cell compartments PrP-KO CGNs respond to the stimulus with significantly larger $[Ca^{2+}]$ transients than PrP-expressing neurons. This is particularly evident in the sub-PM domains and the mitochondrial matrix, where the peak value of $[Ca^{2+}]$ is almost 60% higher in the absence of PrP^C. Values are mean ± SEM; n = 69 (Tg46) and 60 (PrP-KO) in (A), n = 28 (Tg46) and 27 (PrP-KO) in (B), n = 22 (Tg46) and 20 (PrP-KO) in (C); biological replicates were 20 (Tg46) and 18 (PrP-KO) in (A), 10 (for both Tg46 and PrP-KO) in (B), 9 (Tg46) and 8 (PrP-KO) in (C). *******$p<10^{-19}$; ****$p<10^{-5}$; **$p<0.01$ Student's t-test. Other experimental details are as in the legend to Figure 4.

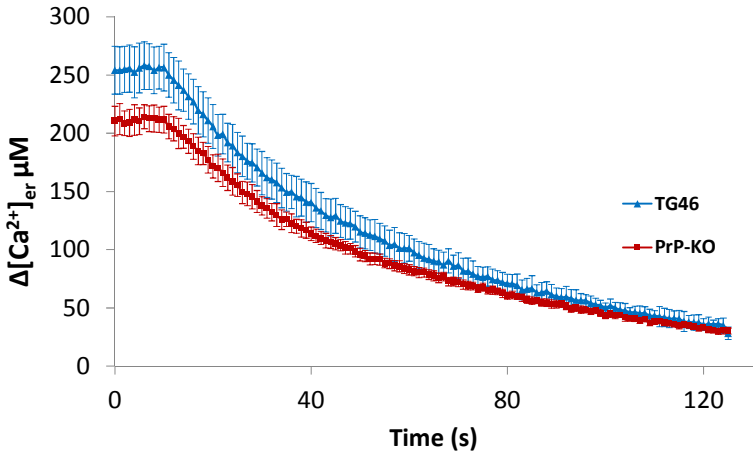

Figure 7. Following the activation of mGLURs, IP_3-mediated Ca^{2+} release from the ER is similar in PrP-KO and Tg46 CGNs.

After the refilling of ER stores (see Figure 5), erAEQ-expressing Tg46 (blue) and PrP-KO (red) CGNs were stimulated with Ca^{2+}-free KRB containing glutamate (100 µM) and EGTA (100 µM). Under these conditions, no contribution is given to ER Ca^{2+} movements by the entry of Ca^{2+} into the cell through PM ionotropic GluRs, and the net Ca^{2+} release from the ER through IP_3-sensitive channels can be monitored. No significant difference in the rate of Ca^{2+} release from ER stores is observed between PrP-KO and PrP-expressing neurons. Reported traces are mean ± SEM; n = 9 for both Tg46 and PrP-KO; biological replicates were 3 for both mouse strains. Other experimental details are as in the legend to Figure 5.

3.3.3 INVOLVEMENT OF PrP^C IN LOCAL Ca^{2+} MOVEMENTS INDUCED BY STIMULATION OF NMDA-SENSITIVE RECEPTORS

After monitoring local Ca^{2+} fluxes elicited by stimulation of all glutamate-sensitive receptors and preferentially mGLUR-induced ER Ca^{2+} release, we examined the contribution of ionotropic GluRs to Ca^{2+} homeostasis of PrP-KO and Tg46 CGN. Specifically, we focused on NMDARs in light of the recent evidence that, by binding the NR2D subunit, PrP^C diminishes Ca^{2+} entry through NMDA-sensitive GluRs (Khosravani *et al.,* 2008). The NMDAR is obligatory composed by two NR1 subunits that co-assemble with other two (NR2) subunits to form the mature, active tetrameric

channel complex permeable to both Na^+ and Ca^{2+}. The NR2 subunit exists in various isoforms (A-B-C-D) that determine the activity of NMDARs, with the NR2D subunit showing much slower kinetic properties compared with the other subunits (e.g., NR2B) (Cull-Candy and Leszkiewicz, 2004).

To stimulate NMDAR, we used CGN after SOCCs-induced Ca^{2+} measurements were completed as previously described. CGN were perfused with KRB containing Ca^{2+} (1 mM), NMDA (50 μM) and its co-agonist glycine (10 μM), and Ca^{2+} transients were monitored using pmAEQ, cytAEQ or mtAEQ. As shown (Fig. 8), activation of NMDARs induced Ca^{2+} transients that in both plasma membrane (Fig. 8A) and cytosolic (Fig. 8B) domains of PrP-KO CGN were higher than in Tg46 neurons by 100% and 25%, respectively (peak values: in PM domains, 2.14 ± 0.11 μM, PrP-KO CGN and 1.04 ± 0.06 μM, Tg46 CGN; in cytosol, 1.33 ± 0.14 μM, PrP-KO and 1.07 ± 0.04 μM, Tg46). This result is in line with the above-mentioned electrophysiological data obtained by Khosravani *et al.* (2008) in hippocampal neurons. In contrast, when mitochondrial Ca^{2+} transients were followed, we found that PrP-KO CGN (40.67 ± 2.92 μM) accumulated 30% less Ca^{2+} than control cells (57.28 ± 6.00 μM) (Fig. 8C). This result means that NMDAR-mediated Ca^{2+} influx cannot explain the higher mitochondrial Ca^{2+} peak value displayed by PrP-KO CGN after activation of all glutamate receptors (Fig. 6C). Given that this value can neither be attributed to a higher IP_3-mediated Ca^{2+} released by PrP-KO CGNs (Fig. 7), we are left with the possibility that a specific contribution by AMPARs and/or kainate receptors takes place in PrP-KO neurons. This hypothesis, however, still awaits confirmation.

Finally, a comment is due to the fact the protocol used by us to maximally stimulate NMDARs could not faithfully reproduce the physiological situation. Indeed, in addition to glutamate, the *in vivo* activity of NMDARs is likely to be strongly influenced by the activity of mGluRs, some subtypes of which are known to trigger signaling pathways, e.g., Pyk2/CAKβ and Src-family kinases, which may ultimately upregulate NMDAR activity (Manzerra *et al.*, 2002).

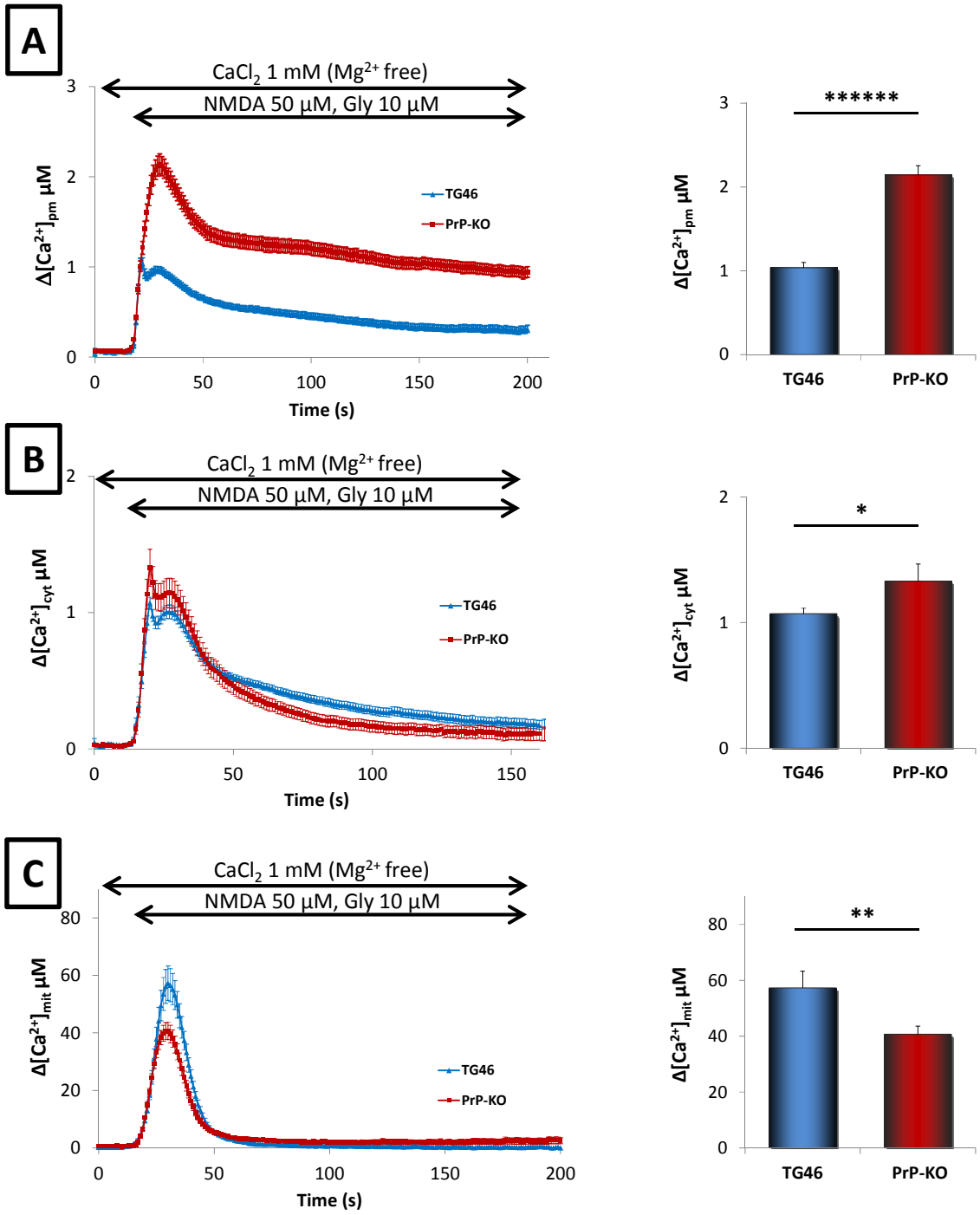

Figure 8. Activation of NMDA (ionotropic) glutamate receptors elicits $[Ca^{2+}]_{pm}$, $[Ca^{2+}]_{cyt}$, and $[Ca^{2+}]_{mit}$ transients that are significantly different in PrP-KO CGNs with respect to Tg46 neurons

Tg46 (blue) and PrP-KO (red) CGNs expressing pmAEQ (A), cytAEQ (B), or mtAEQ (C) were stimulated with NMDA (50 µM) and glycine (10 µM) in a Mg^{2+}-free, $CaCl_2$ (1 mM)-supplemented buffer. This protocol provokes the activation of NMDARs at the PM, and transient $[Ca^{2+}]$ rises in the different cell domains that were recorded by means of the targeted AEQ probes. Both the mean of the recorded traces (left panels), and the peak values reported in the bar diagrams (right panels) show that in sub-PM domains and bulk cytosol PrP-KO neurons have increased Ca^{2+} responses with respect to the PrP-expressing counterpart. Noteworthy, the response of PrP-KO CGNs is also characterized by a prolonged pseudo-steady-state that

sustains the presence of abnormally high Ca^{2+} levels at the sub-PM domains for hundreds of seconds after the beginning of the stimulus. On the contrary, the NMDA-induced mitochondrial Ca^{2}+ uptake is significantly lower in PrP-KO than in Tg46 CGNs. Values are mean ± SEM; n = 71 (Tg46,) and 68 (PrP-KO) in (A), n = 24 (Tg46) and 22 (PrP-KO) in (B), n = 17 (Tg46) and 28 (PrP-KO) in (C); biological replicates were 17 for both Tg46 and PrP-KO in (A), 10 (Tg46) and 9 (PrP-KO) in (B), 7 (Tg46) and 11 (PrP-KO) in (C). ******$p<10^{-14}$; **p<0.01; *p<0.05 Student's t-test. Other experimental details are as in the legend to Figure 6.

3.3.4 ANALYSIS OF $p59^{Fyn}$ AND p42/44-ERK ACTIVATION IN Tg46 AND PrP-KO CGN

An obvious question raised by the previous results concerns the mechanism(s) through which PrP^{C} can modulate cell Ca^{2+} homeostasis, in particular Ca^{2+} entry through SOCCs and NMDARs. As for NMDAR modulation by PrP^{C}, a direct physical and functional interaction between the two proteins has been already demonstrated, whereby PrP^{C} would bind to, and inhibit, NMDAR subunit NR2D, thus reducing NMDA-mediated Ca^{2+} entry (Khosravani *et al.*, 2008). In addition, a previous study in the laboratory in which this work has been carried out has demonstrated that the higher Ca^{2+} transients observed in PrP-KO CGNs can be (at least in part) explained by the reduced expression in these neurons of two important systems deputed to the extrusion of Ca^{2+} from the cytosol (i.e., PMCA and SERCA) compared to the PrP-expressing counterpart (Lazzari *et al.*, 2011). Notably, the reduction of SERCA amounts in PrP-KO neurons also nicely fits with the lower steady-state level of $[Ca^{2+}]_{er}$ reported here (Figure 5). In this work, we have decided to verify whether PrP^{C} could impinge on Ca^{2+}-transporting mechanisms through the regulation of specific cell signaling pathways, namely those involving SFKs (*Src* family of tyrosin kinases) (in particular, $p59^{Fyn}$ that is the *Srk* kinase prevalently expressed in CGNs), and p42/p44-ERK (ERK1/2), belonging to the family of mitogen-activated protein (MAP) kinases. This choice stems from two principles. On one hand, it is known that $p59^{Fyn}$ and ERK1/2 are involved in the regulation of both SOCC and NMDAR activity (Babnigge *et al.*, 1997; El-Yassim *et al.*, 2008; Nakazawa *et al.*, 2001; Suzuki and Okumura-Noji, 1995; Kohno *et al.*, 2008; Pozo-Guisado *et al.*, 2010). On the other hand, PrP^{C} has been repeatedly suggested to participate in signal transduction mechanisms at the cell surface impinging on both $p59^{Fyn}$ and ERK1/2 pathways (for reviews, see Linden *et al.*, 2008; Sorgato *et al.*, 2009). Moreover, it is good to remind that these two signaling pathways are closely related, given that ERK1/2 activation can be also mediated by $p59^{Fyn}$ through the Ras/Raf pathway (Ramos, 2008).

We scrutinized the phosphorylation levels of $p59^{Fyn}$ and ERK1/2 under steady-state conditions after prolonged incubation in either a Ca^{2+}-free medium containing EGTA (100 μM), or a Ca^{2+}-

containing (1 mM) medium, thus mimicking the state in which neurons were just before SOCE or glutamate/NMDA stimulation, respectively. As shown in Figure 9, $p59^{Fyn}$ activation was higher (~30%) in PrP-KO CGN compared to Tg46 neurons, before both SOCE and glutamate/NMDA stimulation, whereas ERK1/2 phosphorylation was significantly increased in the PrP-KO genotype (~60% more than Tg46 CGNs) only when neurons were kept in the Ca^{2+}-containing medium (Figure 10). These findings thus support the possibility that $p59^{Fyn}$- and ERK1/2-regulated signaling pathways act as intermediate players between PrP^{C}, and SOCC- and/or glutamate/NMDA-mediated Ca^{2+} movements.

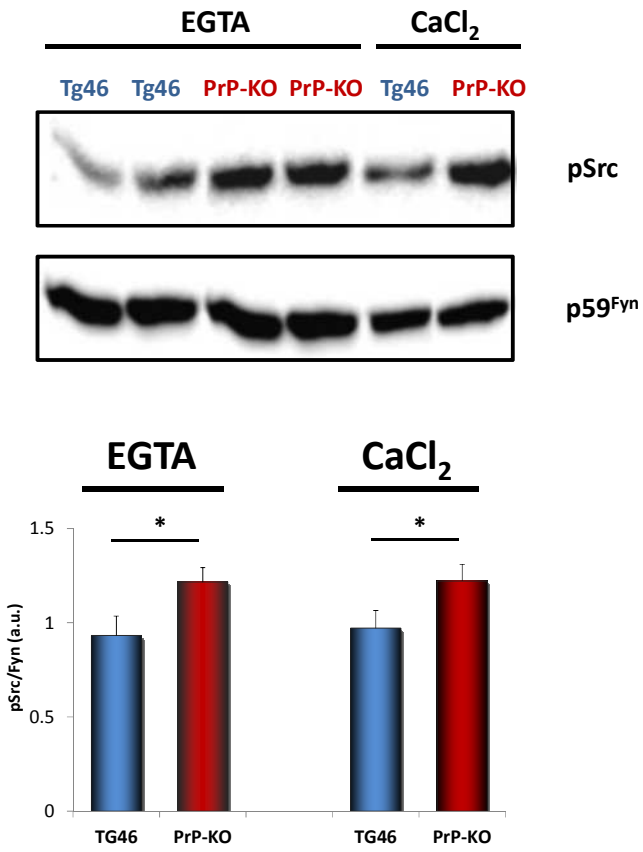

Figure 9. $p59^{Fyn}$ phosphorylation is higher in PrP-KO than in Tg46 CGNs after incubation in both the Ca^{2+}-free and Ca^{2+}-containing medium.

Tg46 (blue) and PrP-KO (red) CGNs, subjected to treatments mimicking those occurring before either SOCE (EGTA 100 µM, see Figure 4), or glutamate/NMDA stimulation (Ca^{2+} 1 mM , see Figures 6 and 8), were harvested and homogenized, and then subjected to Western blot analysis for quantifying the phosphorylation state of $p59^{Fyn}$, as described under Materials and Methods. The upper panel reports a Western blot representative of 10 independent experiments for each PrP genotype, while the lower panel reports the densitometric analysis of anti-p-Src immunosignals (with an Ab directed to the activatory phosphorylated site Y416 of $p59^{Fyn}$), normalized to the density of total $p59^{Fyn}$ immunoreactive bands, under the indicated experimental conditions. Shown data indicates that $p59^{Fyn}$ is significantly more active (~30%) in PrP-KO CGNs compared to the PrP-expressing counterpart, under both Ca^{2+}-free and Ca^{2+}-rich

conditions. Values are mean ± SEM; n = 10 for both the Tg46 and PrP-KO genotypes and the cell treatment protocols. *p<0.05 Student's t-test.

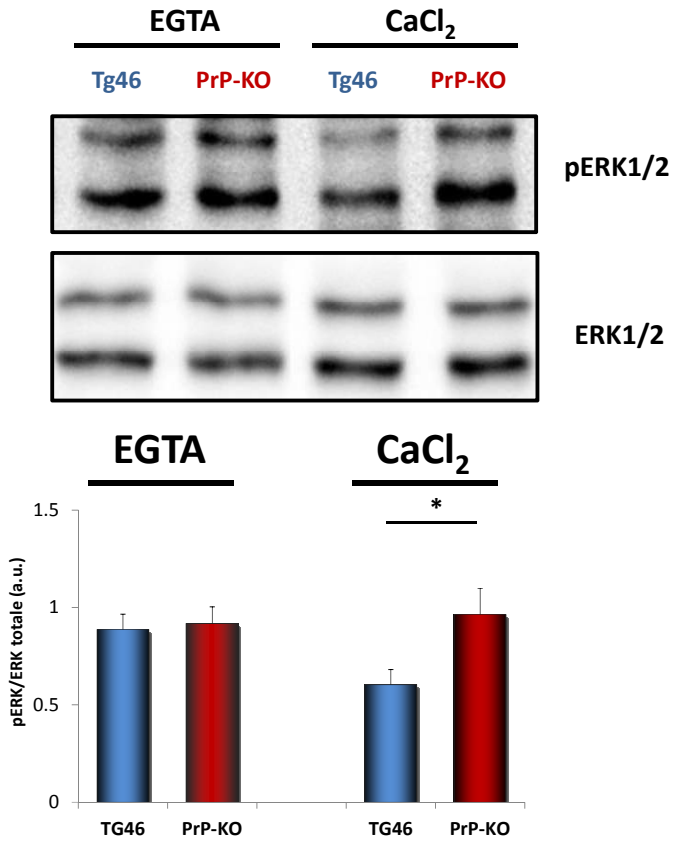

Figure 10. ERK1/2 MAP kinases are more phosphorylated (active) in PrP-KO than in Tg46 CGNs after incubation in the Ca^{2+}-containing, but not in the Ca^{2+}-free, medium.

Tg46 and PrP-KO CGNs were subjected to Western blot analysis for quantifying the phosphorylation state of ERK1/2. The upper panel reports a Western blot representative of 10 independent experiments for each PrP genotype, while the lower panel reports the densitometric analysis of anti-p-ERK1/2 over total ERK1/2 immunoreactive bands, under the indicated experimental conditions. Shown data indicates that ERK1/2 is significantly more active (~60%) in PrP-KO CGNs compared to the PrP-expressing counterpart under conditions mimicking those occurring before glutamate/NMDA stimulation (Ca^{2+} 1 mM), but not before SOCE (EGTA 100 μM). Values are mean ± SEM; n = 10 for both the Tg46 and PrP-KO genotypes and the cell treatment protocols. *p<0.05 Student's t-test. Other experimental details are in the legend to Figure 9.

Taken together, shown results demonstrate that PrP^C play a role in neuronal Ca^{2+} homeostasis, modulating Ca^{2+} transients elicited by different stimuli in different cell domains/compartments. With the exception of the steady-state level of the ER lumen, in which $[Ca^{2+}]$ is significantly lower when PrP^C is absent, PrP^C seems to have the general role to limit Ca^{2+} rises inside neurons, in particular in the cytosol and the mitochondrial matrix, when neurons are exposed to SOCE or glutamate/NMDA. This underscores a possible important role for PrP^C in maintaining a correct neuronal Ca^{2+} homeostasis and, consequently, normal cell excitability and synaptic functions. Such a synaptic role for PrP^C has also been demonstrated by other studies, showing that its absence provoked deficits in spatial learning (Criado *et al.*, 2005), altered long-term potentiation (Collinge *et al.*, 1994; Maglio *et al.*, 2004; Manson *et al.*, 1995), and increased neuronal excitability (Colling *et al.*, 1996; Mallucci *et al.*, 2002). Our findings are also in line with the alleged neuroprotective role ascribed to the protein, given that intracellular Ca^{2+} overloads are commonly associated to neuronal damage and death. The fact that alterations of Ca^{2+}-dependent neuronal functions were observed in prion disease models (Peggion *et al.*, 2011), in which functional PrP^C is continuously converted into PrP^{Sc}, also allows us to propose a suggestive perspective, in which the control of Ca^{2+} homeostasis is a therapeutic target for prion diseases.

By a molecular point of view, we have demonstrated that PrP^C could exert its control over neuronal Ca^{2+} homeostasis by modulating important intracellular signaling pathways, i.e., those involving $p59^{Fyn}$ and ERK1/2. Further studies are required, however, to elucidate better this issue, such as investigations implicating the pharmacologic inhibition of these pathways, and/or focused on the phosphorylation pattern of components of the SOCE machinery and of glutamate/NMDA receptors.

3.4 TREATMENT OF CGN WITH Aβ OLIGOMERS

The amyloid Aβ peptide (in particular the 1-42 amino acid-long species) is produced by the proteolysis of APP. It shows a remarkable ability to aggregate, leading to the formation of large and insoluble deposits (plaques) in the brain of patients affected by AD (Glenner and Wong, 1984). The "amyloid cascade hypothesis" postulates that a time-dependent deposition of Aβ aggregates in the brain is responsible for AD neurodegeneration (Hardy and Higgins, 1992). Several recent evidences, however, suggest that instead of large amyloids the toxic species responsible for AD cognitive and functional derangement are soluble Aβ oligomers, known as Aβ-derived diffusible ligands (ADDLs) (Lambert *et al.*, 1998; Lacor *et al.*, 2004; Cleary *et al.*, 2005).

To ascertain whether a PrP^C-dependent distortion of Ca^{2+} homestasis could be involved in the Aβ oligomer-induced neurodegeneration occurring in AD, primary cultures of CGNs with different PrP genotypes were treated with Aβ oligomers and then assayed for local Ca^{2+} movements (by the AEQ-based strategy). Given that the high Aβ propensity to aggregate, and its low *in vivo* concentration (nM) preclude isolation of large quantities of soluble Aβ peptides from natural sources (Hepler *et al.*, 2006), we have used chemically synthesized Aβ1-42 fragments that were subsequently subjected to an oligomerization process.

3.4.1 CHARACTERIZATION OF Aβ PEPTIDES

To qualitatively characterize the used preparations, Aβ1-42 samples were analyzed by Western blot (using anti-Aβ 6E10 mAb) before and after the oligomerization process. As shown in Fig. 9, the Aβ1-42 peptide (of approximately 4.5 KDa molecular mass in its monomeric form) migrates in different oligomerized forms, from monomers, to dimers, to trimers, and higher order-oligomers. This pattern is observed both before (line 1), and after (line 2) the so-called process of "aging" (37°C, 1 h), although the "aging" treatment clearly increases the amount of high mass species over the lower mass ones predominating in the freshly diluted Aβ preparations. This result indicates that the process of oligomerization is effective, although more sophisticated investigations, e.g. by size-exclusion chromatography, are necessary to provide a definitive profile of the oligomeric/aggregated states.

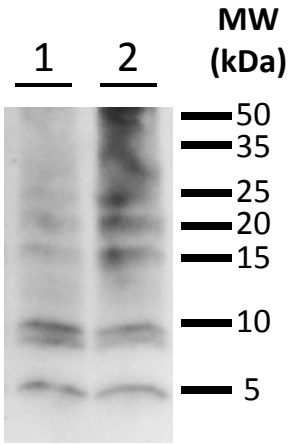

Figure 11. The procedure of Aβ1-42 oligomerization increases the abundance of n-mers of higher molecular weight with respect to freshly dissolved peptide preparations. Chemically-synthesized Aβ1-42 peptide samples were subjected, or not, to the process of oligomerization described in Materials and Methods. The qualitative analysis of the peptide preparations by Western blot (using anti-Aβ mAb 6E10) demonstrates that, while freshly resuspended Aβ peptides were mainly present as monomers (~5 kDa) and dimers (lane 1), after the oligomerization step the immuno-reactive signal was enriched in 3-mers, and higher order-oligomers (lane 2). Molecular mass standards (kDa) are reported on the right.

3.4.2 EFFECTS OF Aβ OLIGOMERS IN CGN LOCAL [Ca^{2+}] MOVEMENTS

We then investigated whether Aβ1-42 oligomers were affecting local Ca^{2+} fluxes in a PrP^C-dependent manner. To this end, CGN (with or without PrP^C) expressing each AEQ isoform were subjected to protocols identical to those reported above but for the presence of Aβ1-42 fragments (5 μM).

In this thesis, we show only the data obtained after about SOCCs stimulation in light of the good number of experiments carried out. Conversely, we unfortunately have not yet accumulated a similar number of experiments using glutamate or by stimulating specifically NMDARs.

LOCAL [Ca^{2+}] CHANGES AFTER Ca^{2+} ENTRY THROUGH SOCCs

We first examined Ca^{2+} fluxes through SOCCs using pmAEQ (Fig. 10A). We found that, compared to the untreated counterpart, addition of Aβ1-42 oligomers to Tg46 CGN induced a statistically significant (20%) increase of Ca^{2+} peak transients in PM microdomains (light blue bar) (peak values: 21.41 ± 0.56 μM, (untreated) Tg46 CGN; 26.27 ± 2.07 μM, Tg46 CGN +Aβ(1-42)). These results favor the assumption that the interaction of PrP^C with Aβ peptides distorts the function of PrP^C. Indeed, were the control exerted by PrP^C over SOCE lost after Aβ addition, Tg46 CGN

should have increased Ca^{2+} transients similar to (untreated) PrP-KO neurons. This is indeed the trend displayed by Aβ–treated Tg46 CGN. On the same basis, PrP-KO neurons should not have been affected by Aβ oligomers. Instead, we observed a decreased Ca^{2+} transient (pink bar) that, although not statistically significant, likely indicates an unspecific effect of Aβ peptides on neuronal plasma membrane permeability (peak values: 30.40 ± 1.48 μM, (untreated) PrP-KO CGN; 25.93 ± 1.36 μM, PrP-KO CGN +Aβ(1-42)). It is important to consider that, were this effect real, it means that the 20% increase observed in Aβ-treated Tg46 CGN would be much higher, being it masked by the unspecific effect that can be observed in the absence of PrP^C. To note that in the original paper demonstrating that PrP^C acts as Aβ-receptor, it was reported that this role accounts for only 50% of toxic Aβ effects in neurons (Laurén *et al.*, 2009).

Next, we investigated how the cytosol and the mitochondrial matrix reacted to SOCC-mediated Ca^{2+} influx in the presence of Aβ oligomers. As shown, Aβ oligomers did not provoke any variation of Ca^{2+} transients neither in the cytosol (light blue bar, Fig. 10B) nor (as expected in light of Fig. 10B) in the mitochondrial matrix (light blue bar, Fig. 10C) of Tg46 CGN (peak value: in cytosol, 1.08 ± 0.05 μM, (untreated) Tg46 CGN and 1.15 ± 0.11 μM, Tg46 CGN +Aβ(1-42); in mitochondria, 21.84 ± 1.01 μM, (untreated) Tg46 CGN, and 19.96 ± 1.62 μM, Tg46 CGN +Aβ(1-42)). Once again, however, somehow supporting the above reasoning, we found that treatment of PrP-KO CGN significantly decreased Ca^{2+} transients (by approximately 20%) in both domains (pink bars of Fig. 10B and 10C, respectively) (peak value: in cytosol, 1.26 ± 0.06 μM, (untreated) PrP-KO CGN and 1.00 ± 0.03 μM, PrP-KO CGN +Aβ(1-42); in mitochondria, 26.11 ± 0.93 μM, (untreated) PrP-KO CGN and 19.60 ± 1.78 μM, PrP-KO CGN +Aβ(1-42)).

Notwithstanding the difficulty of interpretation that is augmented by the notion that the absence of PrP^C is itself perturbing Ca^{2+} homeostasis, a rather complex picture emerges from our study on PrP^C as possible mediator of Aβ effects. Regarding SOCE, for which we have accumulated a good number of experiments, data obtained in neurons expressing or not PrP^C strongly indicate that Aβ oligomers have both a PrP^C-dependent and a PrP^C-independent effect, respectively, and that the latter likely masks the effective impact of PrP^C-Aβ interactions. This allows us to conclude that PrP^C appears to be involved in triggering Aβ-mediated Ca^{2+} dys-homeostasis, at least at the level of SOCE. Concurrently, it reinforces the notion that PrP^C controls SOCE, as proposed (Lazzari *et al.*, 2011).

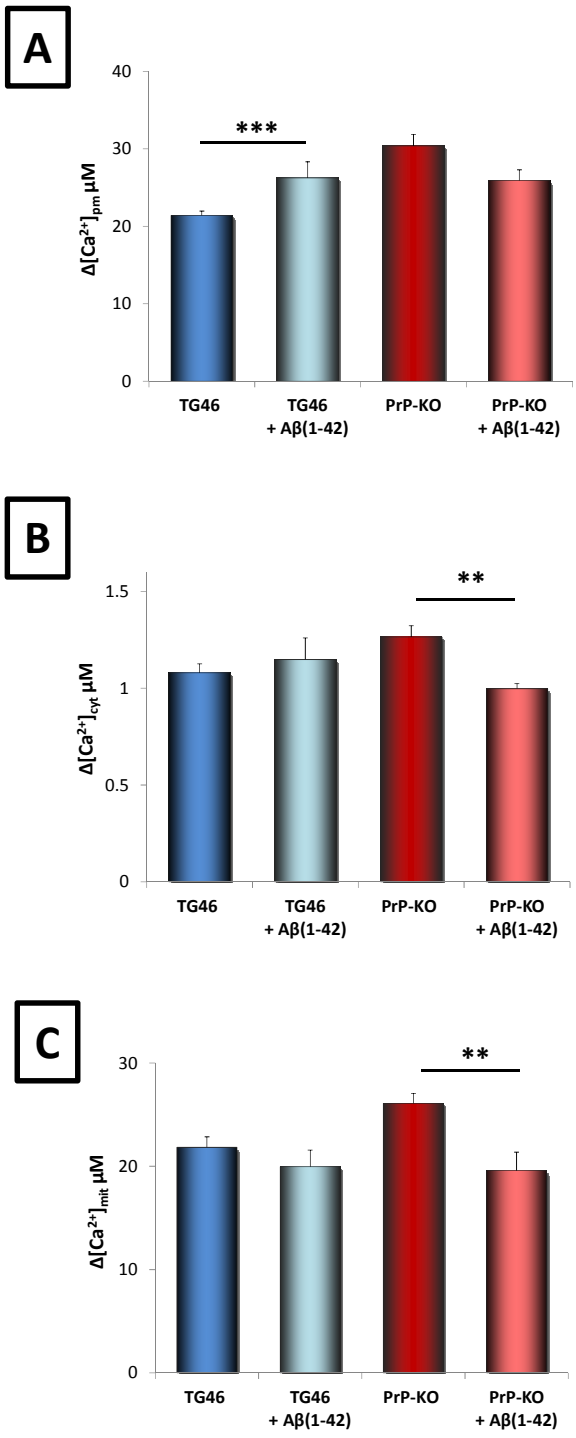

Figure 1210. PrP^C-dependent and -independent effects of oligomerized Aβ1-42 peptides on local SOCE-mediated Ca^{2+} movements.

Tg46 (blue) and PrP-KO (red) CGNs expressing pmAEQ (A), cytAEQ (B), or mtAEQ (C), incubated (light color), or not (dark color), with oligomerized Aβ1-42 peptides were subjected to SOCE stimulation. Bar diagrams report the peak values of the Ca^{2+} transients observed in the different cell domains. While Aβ1-42 induces a prevailing "PrP-independent" reduction of the Ca^{2+} transients in bulk cytosol and the mitochondrial matrix (see the PrP-KO values in panel B and C, respectively), the "PrP-dependent" effect is

able to overcome the PrP-independent one in the sub-PM domains (see the TG46 values in panel A). Values are mean ± SEM; n = 174 (Tg46), 42 (Tg46+Aβ(1-42)), 169 (PrP-KO) and 40 (PrP-KO+Aβ(1-42)) in (A), n = 41 (Tg46), 13 (Tg46+Aβ(1-42)), 57 (PrP-KO) and 18 (PrP-KO+Aβ(1-42)) in (B), n = 56 (Tg46), 18 (Tg46+Aβ(1-42)), 70 (PrP-KO) and 17 (PrP-KO+Aβ(1-42)) in (C). Biological replicates were 20 (for both Tg46 and PrP-KO) or 6 (for both Tg46+Aβ(1-42) and PrP-KO+Aβ(1-42)) in (A); 10 (Tg46), 12 (PrP-KO) or 4 (for both Tg46+Aβ(1-42) and PrP-KO+Aβ(1-42)) (B); 10 (Tg46), 13 (PrP-KO) or 4 (for both Tg46+Aβ(1-42) and PrP-KO+Aβ(1-42)) in (C). ***p<0.001, **p<0.01, Student's t-test. All other details are as described in Materials and Methods and the legend to Figure 4. The mean traces from which the reported peak values were calculated are illustrated in the Supplementary Information section (Figure S1).

3.4.3 TREATMENT WITH Aβ ABOLISHES THE EFFECT OF PrP^C ON THE $p59^{Fyn}$ PATHWAY

In the attempt to rationalize the above findings on molecular basis, we analyzed whether treatment with oligomerized Aβ1-42 affected $p59^{Fyn}$ and Erk1/2 activation (before SOCE stimulation) in a PrP^C-dependent manner. While in the case of Erk1/2 no significant effect was observed (data not shown), Aβ treatment increased the steady-state phosphorylation levels of $p59^{Fyn}$ after incubation of neurons in the Ca^{2+}-free medium, thereby completely abrogating the difference observed in untreated CGNs (Figure 13). Thus, PrP^C-Aβ docking seems to abolish the PrP^C-dependent down-regulation of the $p59^{Fyn}$ pathway, which may in turn stimulate SOCC activation, and promote the larger Ca^{2+} transients that were observed in sub-PM domains (see Figure 12A, and Figure S1 in the Supplementary Information section). Interestingly, it has been recently reported that Aβ binding to PrP^C leads to the phosphorylation of the NMDAR subunit NR2B by activated $p59^{Fyn}$ at the synapses of cortical neurons, with consequent neuronal Ca^{2+} overload and excitotoxicity (Um *et al.*, 2012). It will thus be of major interest to understand whether treatment with Aβ oligomers induces PrP^C-dependent (and $p59^{Fyn}$-mediated) alterations of local Ca^{2+} movements in NMDA-stimulated CGNs.

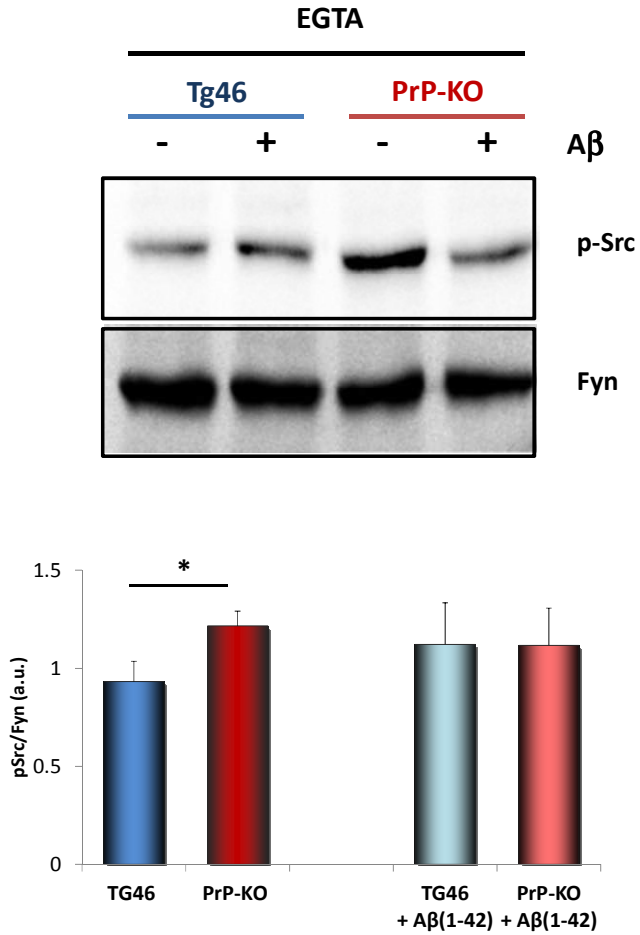

Figure 13. Treatment with Aβ1-42 abrogates the down-regulation of $p59^{Fyn}$ activation by PrP^{C}.
Tg46 (blue) and PrP-KO (red) CGNs, treated, or not, with oligomerized Aβ1-42, subjected to an incubation protocol mimicking that occurring before SOCE (EGTA 100 µM, see Figure 4), were subjected to Western blot analysis for quantifying the phosphorylation state of $p59^{Fyn}$. The upper panel reports a representative Western blot, while the lower panel reports the densitometric analysis, under the indicated experimental conditions. Treatment with Aβ1-42 increases the steady-state phosphorylation levels of $p59^{Fyn}$ and completely abolishes the difference observed in untreated CGNs (cfr. Figure 13). Values are mean ± SEM; n = 10 for untreated CGNs, and n = 4 for Aβ-treated samples. *p<0.05 Student's t-test.

In neurons, maintenance of a proper Ca^{2+} homeostasis is fundamental for many cellular functions, including synaptic activity and memory formation and consolidation, and for cell survival (Mattson, 2007). Of consequence, defects of Ca^{2+} signaling contributes to synaptic dysfunctions, and can lead to excitotoxic and/or apoptotic death, all of which are hallmarks of many neurodegenerative diseases, including AD (Bezprozvanny, 2009). Although the precise mechanisms of AD-related neurodegeneration are not yet known, it is now commonly recognized that it is caused by Aβ peptide oligomeric species. Much credit is also given to the possibility that Aβ-induced disruption of Ca^{2+} homeostasis has a central role in AD pathogenesis (Mattson and Chan, 2003).

Given that PrP^C is involved in Ca^{2+} homeostasis (Lazzari et al., 2011; for a review see Peggion *et al.*, 2011), and may act as a high-affinity receptor for Aβ oligomers (Laurén *et al.*, 2009; Balducci *et al.*, 2010; Calella *et al.*, 2010; Chen *et al.*, 2010; Freir *et al.*, 2011; Zou *et al.*, 2011), possibly mediating their neurotoxic effects (Laurén *et al.*, 2009; Chen *et al.*, 2010; Chung *et al.*, 2010; Gimbel *et al.*, 2010; Alier *et al.*, 2011; Barry *et al.*, 2011; Bate and Williams, 2011; Freir *et al.*, 2011; Resenberger *et al.*, 2011; Zou *et al.*, 2011; Kudo *et al.*, 2012; Um *et al.*, 2012; You *et al.*, 2012), we have investigated whether PrP^C-Aβ binding perturbs local Ca^{2+} homeostasis in neurons. This was indeed what we have found with respect to SOCE. Intriguingly, treatment with Aβ increased Ca^{2+} transients in sub-PM domains of PrP-expressing CGNs (Figure 12A), thereby completely abrogating the differences between these neurons and the PrP-KO counterpart. A similar effect was observed with respect to activated $p59^{Fyn}$ levels (Figure 13), suggesting that the binding of Aβ1-42 oligomers diverts the normal PrP^C function, mimicking a PrP-KO phenotype. Abrogation of the differences displayed by PrP-KO and TG46 neurons with respect to SOCE-mediated Ca^{2+} fluxes seems to be a general action of Aβ oligomers, given that this was also observed for Ca^{2+} fluxes in the cytosol and in the mitochondrial matrix. In these cases, however, this was due to a reduced response of Aβ-treated PrP-KO neurons compared to the untreated counterpart (Figure 12B and C), to explain which one needs to invoke PrP-independent effects of Aβ oligomers on SOCE. This is not surprising, given that it was previously found that only about 50% of Aβ oligomers bind to neurons in a PrP^C-dependent manner (Lauren et al., 2009).

We now know that, in AD, glutamatergic neurotransmission – fundamental to learning and memory – is severely disrupted. In particular, Aβ oligomers may promote excessive activation of glutamate receptors, and the consequent Ca^{2+} overload may lead to neuronal dysfunction and cell death (Mattson and Chan, 2003). Although glutamate can be neurotoxic through excessive stimulation of both ionotropic and metabotropic glutamate receptors, disruption of neuronal

functions in AD seems to depend primarily on NMDAR activation (Butterfield and Pocernich, 2003). In this context, it has been reported that Aβ oligomers affect – through both direct and indirect mechanisms – NMDARs by keeping its ion channel tonically open. By causing excessive Ca^{2+} influx, this leads to impairment of synaptic plasticity, LTP and learning/memory, and eventually neuronal death (Danysz and Parsons, 2012). Hopefully, the role of PrP^{C} in mediating Ca^{2+}-dependent toxic effects of Aβ oligomers will be better understood once our experiments involving glutamate and NMDA stimulation of CGNs will be completed.

SUPPLEMENTARY INFORMATION

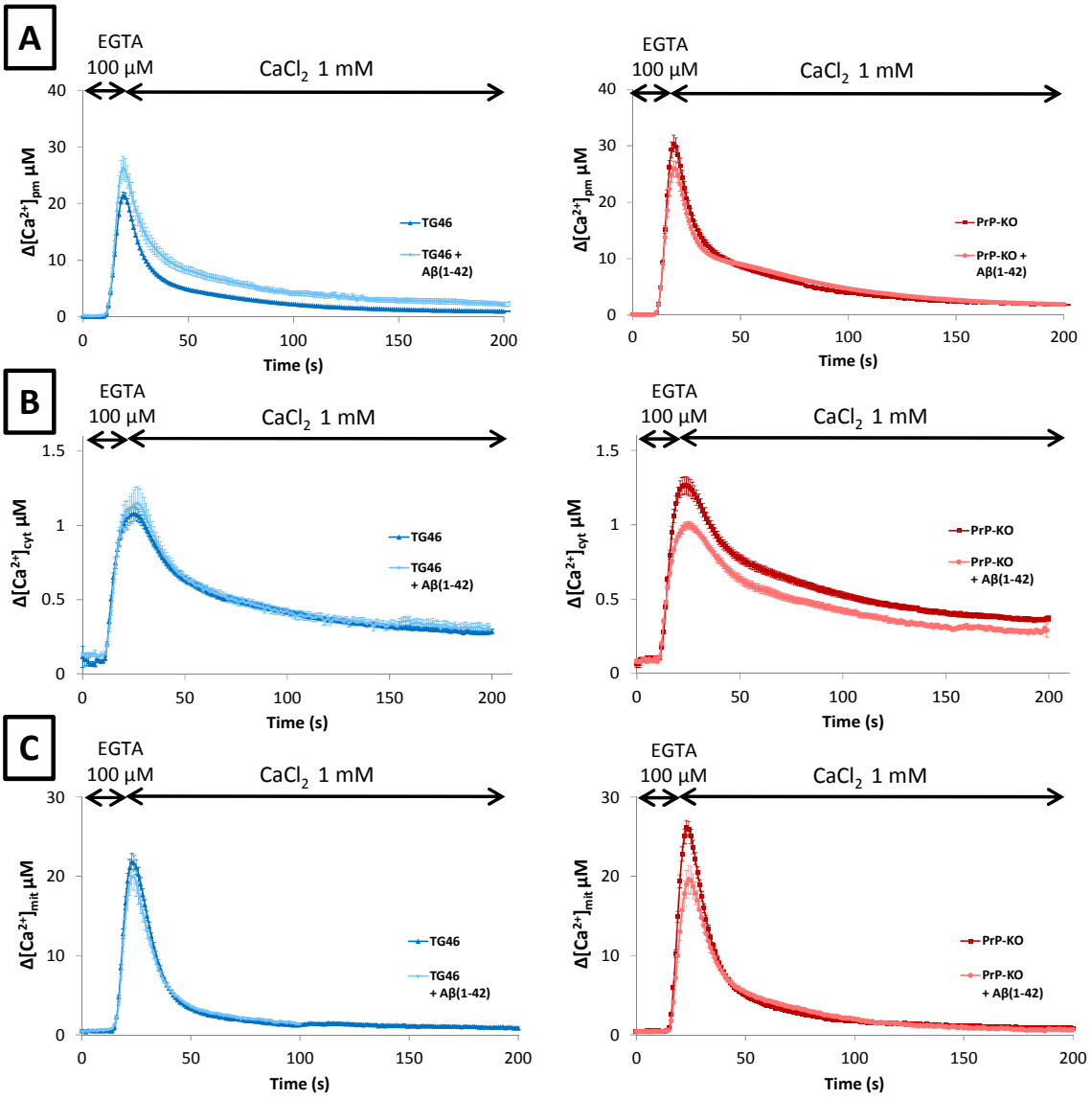

Figure S111. PrP^{C}-dependent and -independent effects of oligomerized Aβ1-42 peptides on local SOCE-mediated Ca^{2+} movements.

Tg46 (blue) and PrP-KO (red) CGNs expressing pmAEQ (A), cytAEQ (B), or mtAEQ (C), incubated (light color), or not (dark color), with oligomerized Aβ1-42 peptides were subjected to SOCE stimulation. The figure reports the mean traces of the observed Ca^{2+} transients whose peak values are reported in Figure 12. See Figure 12 for all experimental details and statistics.

REFERENCES

Aguzzi A., Baumann F., and Bremer J. (2008). The prion's elusive reason for being. *Annu. Rev. Neurosci.* **31**, 439–477.

Aguzzi A., and Calella A.M. (2009). Prions : protein aggregation and infectious diseases. *Physiol. Rev.* **89**, 1105–1152.

Alier K., Ma L., Yang J., Westaway D., and Jhamandas J.H. (2011). Aβ inhibition of ionic conductance in mouse basal forebrain neurons is dependent upon the cellular prion protein PrPC. *J. Neurosci.* **31**, 16292–16297.

Alper T., Cramp W.A., Haig D.A., and Clarke M.C. (1967). Does the agent of scrapie replicate without nucleic acid? *Nature* **214**, 764–766.

Alper T., Haig D.A., and Clarke M.C. (1966). The exceptionally small size of the scrapie agent. *Biochem. Biophys. Res. Commun.* **22**, 278–284.

Alzheimer A. (1907). Über eine eigenartige Erkrankung der Hirnrinde. *Allgemeine Zeitschrift Fur Psychiatrie Und Psychisch-gerichtliche Medizin* **64**, 146–148.

Antonyuk S.V., Trevitt C.R., Strange R.W., Jackson G.S., Sangar D., Batchelor M., Cooper S., Fraser C., Jones S., Georgiou T., Khalili-Shirazi A., Clarke A.R., Hasnain S.S., and Collinge J. (2009). Crystal structure of human prion protein bound to a therapeutic antibody. *Proc. Natl. Acad. Sci. USA* **106**, 2554–2558.

Babnigg G., Bowersox S.R., and Villereal M.L. (1997). The role of pp60c-src in the regulation of calcium entry via store-operated calcium channels. *J. Biol. Chem.* **272**, 29434–29437.

Balducci C., Beeg M., Stravalaci M., Bastone A., Sclip A., Biasini E., Tapella L., Colombo L., Manzoni C., Borsello T., Chiesa R., Gobbi M., Salmona M., and Forloni G. (2010). Synthetic amyloid-beta oligomers impair long-term memory independently of cellular prion protein. *Proc. Natl. Acad. Sci. USA* **107**, 2295–2300.

Barry A.E., Klyubin I., Mc Donald J.M., Mably A.J., Farrell M.A., Scott M., Walsh D.M., and Rowan M.J. (2011). Alzheimer's disease brain-derived amyloid-β- mediated inhibition of LTP in vivo is prevented by immunotargeting cellular prion protein. *J. Neurosci.* **31**, 7259–7263.

Basler K., Oesch B., Scott M., Westaway D., Wälchli M., Groth D.F., McKinley M.P., Prusiner S.B., and Weissmann C. (1986). Scrapie and cellular PrP isoforms are encoded by the same chromosomal gene. *Cell* **46**, 417–428.

Bate C., and Williams A. (2011). Amyloid-β-induced synapse damage is mediated via cross-linkage of cellular prion. *J. Biol. Chem.* **286**, 37955–37963.

Beraldo F.H., Arantes C.P., Santos T.G., Machado C.F., Roffe M., Hajj G.N., Lee K.S., Magalhaes A.C., Caetano F.A., Mancini G.L., Lopes M.H., Americo T.A., Magdesian M.H., Ferguson S.S., Linden R., Prado M.A., and Martins V.R. (2011). Metabotropic glutamate receptors transduce

signals for neurite outgrowth after binding of the prion protein to laminin c1 chain. *FASEB J.* **25**, 265–279.

Berridge M.J., Bootman M.D., and Roderick H.L. (2003). Calcium signalling: dynamics, homeostasis and remodelling. *Nat. Rev. Mol. Cell. Biol.* **4**, 517–529.

Bezprozvanny I. (2009). Calcium signaling and neurodegenerative. *Trends Mol. Med.* **15**, 89–100.

Bolton D.C., McKinley M.P., and Prusiner S.B. (1982). Identification of a protein that purifies with the scrapie prion. *Science* **218**, 1309–1311.

Bremer J., Baumann F., Tiberi C., Wessig C., Fischer H., Schwarz P., Steele A.D., Toyka K.V., Nave K.A., Weis J., and Aguzzi A. (2010). Axonal prion protein is required for peripheral myelin maintenance. *Nat. Neurosci.* **13**, 310–318.

Brini M., Marsault R., Bastianutto C., Alvarez J., Pozzan T., and Rizzuto R. (1995). Transfected aequorin in the measurement of cytosolic Ca2+ concentration ([Ca2+]c). *J. Biol. Chem.* **270**, 9896–9903.

Brini M., Miuzzo M., Pierobon N., Negro A., and Sorgato M.C. (2005). The prion protein and its paralogue Doppel affect calcium signaling in Chinese hamster ovary cells. *Mol. Biol. Cell.* **16**, 2799–2808.

Butterfield D.A., and Pocernich C.B. (2003). The glutamatergic system and Alzheimer's disease - therapeutic implications. *CNS Drugs* **17**, 641–652.

Béranger F., Mangé A., Goud B., and Lehmann S. (2002). Stimulation of PrP(C) retrograde transport toward the endoplasmic reticulum increases accumulation of PrP(Sc) in prion-infected cells. *J. Biol. Chem.* **277**, 38972–38977.

Büeler H., Fischer M., Lang Y., Bluethmann H., Lipp H.P., DeArmond S.J., Prusiner S.B., Aguet M., and Weissmann C. (1992). Normal development and behaviour of mice lacking the neuronal cell-surface PrP protein. *Nature* **356**, 577–582.

Cabral A.L., Lee K.S., and Martins V.R. (2002). Regulation of the cellular prion protein gene expression depends on chromatin conformation. *J. Biol. Chem.* **277**, 5675–5682.

Cahalan M.D. (2009). STIMulating store-operated Ca2+ entry. *Nat. Cell Biol.* **11**, 669–677.

Calella A.M., Farinelli M., Nuvolone M., Mirante O., Moos R., Falsig J., Mansuy I.M., and Aguzzi A. (2010). Prion protein and Abeta-related synaptic toxicity impairment. *EMBO Mol. Med.* **2**, 306–314.

Carafoli E. (2005). The symposia on calcium binding proteins and calcium function in health and disease: an historical account, and an appraisal of their role in spreading the calcium message. *Cell Calcium* **37**, 279–281.

Carafoli E., Genazzani A., and Guerini D. (1999). Calcium controls the transcription of its own transporters and channels in developing neurons. *Biochem. Biophys. Res. Commun.* **266**, 624–632.

Carulla P., Bribian A., Rangel A., Gavin R., Ferrer I., Caelles C., Del Rio J.A., and Llorens F. (2011). Neuroprotective role of PrPC against kainate- induced epileptic seizures and cell death depends on the modulation of JNK3 activation by GluR6/7-PSD-95 binding. *Mol. Biol. Cell.* **22**, 3041–3054.

Castilla J., Saá P., Hetz C., and Soto C. (2005). In vitro generation of infectious scrapie prions. *Cell* **121**, 195–206.

Chen S., Yadav S.P., and Surewicz W.K. (2010). Interaction between human prion protein and amyloid-beta (Abeta) oligomers: role of N-terminal residues. *J. Biol. Chem.* **285**, 26377–26383.

Chesebro B., Race R., Wehrly K., Nishio J., Bloom M., Lechner D., Bergstrom S., Robbins K., Mayer L., Keith J.M., Garon J.M., and Haase A. (1985). Identification of scrapie prion protein-specific mRNA in scrapie-infected and uninfected. *Nature* **315**, 331–333.

Chung E., Ji Y., Sun Y., Kascsak R.J., Kascsak R.B., Mehta P.D., Strittmatter S.M., and Wisniewski T. (2010). Anti-PrP C monoclonal antibody infusion as a novel treatment for cognitive deficits in an Alzheimer's disease model mouse. *BMC Neurosci.* **11**, 1–11.

Cissé M., Sanchez P.E., Kim D.H., Ho K., Yu G.Q., and Mucke L. (2011). Ablation of cellular prion protein does not ameliorate abnormal neural network activity or cognitive dysfunction in the J20 line of human amyloid precursor protein transgenic mice. *J. Neurosci.* **31**, 10427–10431.

Citron M. (2010). Alzheimer's disease: strategies for disease modification. *Nature Rev. Drug Disc.* **9**, 387–398.

Cleary J.P., Walsh D.M., Hofmeister J.J., Shankar G.M., Kuskowski M.A., Selkoe D.J., and Ashe K.H. (2005). Natural oligomers of the amyloid-beta protein specifically disrupt cognitive function. *Nat. Neurosci.* **8**, 79–84.

Colby D.W., and Prusiner S.B. (2011). Prions. *Cold Spring Harb. Perspect. Biol.* **1**, 1–22.

Colling S.B., Collinge J., and Jefferys J.G. (1996). Hippocampal slices from prion protein null mice: disrupted Ca(2+)-activated K+ currents. *Neurosci. Lett.* **209**, 49–52.

Collinge J., Whittington M.A., Sidle K.C., Smith C.J., Palmer M.S., Clarke A.R., and Jefferys J.G. (1994). Prion protein is necessary for normal synaptic function. *Nature* **370**, 295–297.

Criado J.R., Sánchez-Alavez M., Conti B., Giacchino J.L., Wills D.N., Henriksen S.J., Race R., Manson J.C., Chesebro B., and Oldstone M.B. (2005). Mice devoid of prion protein have cognitive deficits that are rescued by reconstitution of PrP in neurons. *Neurobiol. Dis.* **19**, 255–265.

Cull-candy S.G., and Leszkiewicz D.N. (2004). Role of Distinct NMDA Receptor Subtypes at Central Synapses. *Sci. STKE* **1**, 1–9.

Cullie J., and Chelle P. (1939). Experimental transmission of trembling to the goat. *Comptes Rendus Des Seances De l'Academie Des Sciences* **208**, 1058–1160.

Danysz W., and Parsons C.G. (2012). Alzheimer's disease, β-amyloid, glutamate, NMDA receptors and memantine-searching for the connections. *Brit. J. Pharmac.* **167**, 324–352.

Deleault N.R., Harris B.T., Rees J.R., and Supattapone S. (2007). Formation of native prions from minimal components in vitro. *Proc. Natl. Acad. Sci. USA* **104**, 9741–9746.

Demuro A., Parker I., and Stutzmann G.E. (2010). Calcium signaling and amyloid toxicity in Alzheimer's disease. *J. Biol. Chem.* **285**, 12463–12468.

Dermaut B., Croes E.A., Rademakers R., Van den Broeck M., Cruts M., Hofman A., Van Duijn C.M., and Van Broeckhoven C. (2003). PRNP Val129 homozygosity increases risk for early-onset Alzheimer's disease. *Ann. Neurol.* **53**, 409–412.

Donne D.G., Viles J.H., Groth D., Mehlhorn I., James T.L., Cohen F.E., Prusiner S.B., Wright P.E., and Dyson H.J. (1997). Structure of the recombinant full-length hamster prion protein PrP(29-231): the N terminus is highly flexible. *Proc. Natl. Acad. Sci. USA* **94**, 13452–13457.

El-Yassim A., Hitchami A., Besnard P., and Khan N.A. (2008). Linoleic acid induces calcium signaling, Src kinase phosphorylation, and neurotransmitter release in mouse CD36-positive gustatory cells. *J. Biol. Chem.* **283**, 12949–12959.

Elferink L.A., and Scheller R.H. (1993). Synaptic vesicle proteins and regulated exocytosis. *J. Cell. Sci. Suppl.* **17**, 75–79.

Fedrizzi L., and Carafoli E. (2011). Ca2+ dysfunction in neurodegenerative disorders : Alzheimer's disease. *Biofactors* **37**, 189–196.

Follenzi A., and Naldini L. (2002). HIV-based vectors. Preparation and use. *Methods Mol. Med.* **69**, 259–274.

Freir D.B., Nicoll A.J., Klyubin I., Panico S., Risse E., Asante E.A., Farrow M.A., Sessions R.B., Saibil H.R., Clarke A.R., Rowan M.J., Walsh D.M., and Collinge J. (2011). Interaction between prion protein and toxic amyloid β assemblies can be therapeutically targeted at multiple sites. *Nat. Comm.* **2**, 1–9.

Gabizon R., McKinley M.P., Groth D., and Prusiner S.B. (1988). Immunoaffinity purification and neutralization of scrapie prion infectivity. *Proc. Natl. Acad. Sci. USA* **85**, 6617–6621.

Gabriel J.M., Oesch B., Kretzschmart H., Scott M., and Prusiner S.B. (1992). Molecular cloning of a candidate chicken prion protein. *Proc. Natl. Acad. Sci. USA* **89**, 9097–9101.

Gajdusek D.C., Gibbs C.J.J., and Alpers M. (1966). Experimental transmission of a kuru-like syndrome to chimpanzees. *Nature* **209**, 794–796.

Gallo V., Kingsbury A., Balazs R., and Jorgensen O.S. (1987). The role of depolarization in the survival and differentiation of cerebellar granule cells in culture. *J. Neurosci.* **7**, 2203–2213.

Gibbs C.J.J., Gajdusek D.C., Asher D.M., Alpers M.P., Beck E., Daniel P.M., and Matthews W.B. (1968). Creutzfeldt-Jakob disease (spongiform encephalopathy): transmission to the chimpanzee. *Science* **161**, 388–389.

Gimbel D.A., Nygaard H.B., Coffey E.E., Gunther E.C., Laurén J., Gimbel Z., and Strittmatter S.M. (2010). Memory impairment in transgenic Alzheimer mice requires cellular prion protein. *J. Neurosci.* **30**, 6367–6374.

Glenner G.G., and Wong C.W. (1984). Alzheimer's disease: Initial report of the purification and characterization of a novel cerebrovascular amyloid protein. *Biochem. Biophys. Res. Commun.* **120**, 885–890.

Goldfarb L.G., Petersen R.B., Tabaton M., Brown P., LeBlanc A.C., Montagna P., Cortelli P., Julien J., Vital C., Pendelbury W.W., and Al. E. (1992). Fatal familial insomnia and familial Creutzfeldt-Jakob disease: disease phenotype determined by a DNA polymorphism. *Science* **258**, 806–808.

Griffith J.S. (1967). Self-replication and scrapie. *Nature* **215**, 1043–1044.

Griffiths H.H., Whitehouse I.J., Baybutt H., Brown D., Kellett K.A., Jackson C.D., Turner A.J., Piccardo P., Manson J.C., and Hooper N.M. (2011). Prion protein interacts with BACE1 protein and differentially regulates its activity toward wild type and Swedish mutant amyloid precursor protein. *J. Biol. Chem.* **286**, 33489–33500.

Haraguchi T., Fisher S., Olofsson S., Endo T., Groth D., Tarentino A., Borchelt D.R., Teplow D., Hood L., Burlingame A., Lycke E., Kobata A., and Prusiner S.B. (1989). Asparagine-linked glycosylation of the scrapie and cellular prion proteins. *Arch. Biochem. Biophys.* **274**, 1–13.

Hardy J.A., and Higgins G.A. (1992). Alzheimer's disease: the amyloid cascade. *Science* **256**, 184–185.

Hepler R.W., Grimm K.M., Nahas D.D., Breese R., Dodson E.C., Acton P., Keller P.M., Yeager M., Wang H., Shughrue P., Kinney G., and Joyce J.G. (2006). Solution state characterization of amyloid -derived diffusible ligands. *Biochemistry* **45**, 15157–15167.

Horiuchi M., Yamazaki N., Ikeda T., Ishiguro N., and Shinagawa M. (1995). A cellular form of prion protein (PrPC) exists in many non-neuronal tissues of sheep. *J. Gen. Virol.* **76**, 2583–2587.

Hornshaw M.P., McDermott J.R., and Candy J.M. (1995). Copper binding to the N-terminal tandem repeat regions of mammalian and avian prion protein. *Biochem. Biophys. Res. Commun.* **207**, 621–629.

Jakob A. (1920). Über eigenartige erkrankungen des zentralnervensystems mit bemerkenswertem anatomischen befunde. *Zeitschrift Für Die Gesamte Neurologie Und Psychiatrie* **64**, 147–228.

Karran E., Mercken M., and De Stroopper B. (2011). The amyloid cascade hypothesis for Alzheimer's disease: an appraisal for the development of therapeutics. *Nat. Rev. Drug Disc.* **10**, 698–712.

Katzman R. (1986). Alzheimer's disease. *New England J. Med.* **314**, 964–973.

Kendall J.M., Dormer R.L., and Campbell A.K. (1992). Targeting aequorin to the endoplasmic reticulum of living cells. *Biochem. Biophys. Res. Commun.* **189**, 1008–1016.

Kessels H.W., Nguyen L.N., Nabavi S., and Malinow R. (2010). The prion protein as a receptor for amyloid-beta. *Nature* **466**, 1–2.

Khachaturian Z.S. (1994). Calcium hypothesis of aging and dementia. *Ann. New York Acad. Sci.* **747**, 1–11.

Khosravani H., Zhang Y., Tsutsui S., Hameed S., Altier C., Hamid J., Chen L., Villemaire M., Ali Z., Jirik F.R., and Zamponi G.W. (2008). Prion protein attenuates excitotoxicity by inhibiting NMDA receptors. *J. Cell. Biol.* **181**, 551–565.

Kohno T., Wang H., Amaya F., Brenner G.J., Cheng J.K., Ji R.R., and Woolf C.J. (2008). Bradykinin enhances AMPA and NMDA receptor activity in spinal cord dorsal horn neurons by activating multiple kinases to produce pain hypersensitivity. *J. Neurosci.* **28**, 4533–4540.

Kudo W., Lee H.P., Zou W.Q., Wang X., Perry G., Zhu X., Smith M.A., Petersen R.B., and Lee H.G. (2012). Cellular prion protein is essential for oligomeric amyloid-β-induced neuronal cell death. *Hum. Mol. Genet.* **21**, 1138–1144.

Lacor P.N., Buniel M.C., Chang L., Fernandez S.J., Gong Y.S., Viola K.L., Lambert M.P., Velasco P.T., Bigio E.H., Finch C.E., Krafft G.A., and Klein W.L. (2004). Synaptic targeting by Alzheimer's-related amyloid beta oligomers. *J. Neurosci.* **24**, 10191–10200.

Lambert M.P., Barlow A.K., Chromy B.A., Edwards C., Freed R., Liosatos M., Morgan T.E., Rozovsky I., Trommer B., Viola K.L., Wals P., Zhang C., Finch C.E., Krafft G.A., and Klein W.L. (1998). Diffusible, nonfibrillar ligands derived from Abeta-42 are potent central nervous system neurotoxins. *Proc. Natl. Acad. Sci. USA* **95**, 6448–6453.

Laurén J., Gimbel D.A., Nygaard H.B., Gilbert J.W., and Strittmatter S.M. (2009). Cellular prion protein mediates impairment of synaptic plasticity by amyloid-beta oligomers. *Nature* **457**, 1128–1132.

Lazzari C., Peggion C., Stella R., Massimino M.L., Lim D., Bertoli A., and Sorgato M.C. (2011). Cellular prion protein is implicated in the regulation of local Ca2+ movements in cerebellar granule neurons. *J. Neurochem.* **116**, 881–890.

Lee I.Y., Westaway D., Smit A.F.A., Wang K., Seto J., Chen L., Acharya C., Ankener M., Baskin D., Cooper C., Yao H., Prusiner S.B., and Hood L.E. (1998). Complete genomic sequence and analysis of the prion protein gene region from three mammalian species. *Genome Res.* **8**, 1022–1037.

Levi G., Aloisi F., Ciotti M.T., and Gallo V. (1984). Autoradiographic localization and depolarization-induced release of acidic amino acids in differentiating cerebellar granule cell cultures. *Brain Res.* **290**, 77–86.

Li J., Browning S., Mahal S.P., Oelschlegel A.M., and Weissmann C. (2010). Darwinian evolution of prions in cell culture. *Science* **327**, 869–872.

Linden R., Martins V.R., Prado M.A.M., Cammarota M., Izquierdo I., and Brentani R.R. (2008). Physiology of the prion protein. *Physiol. Rev.* 673–728.

Lopes M.H., Hajj G.N.M., Muras A.G., Mancini G.L., Castro R.M.P.S., Ribeiro K.C.B., Brentani R.R., Linden R., and Martins V.R. (2005). Interaction of cellular prion and stress-inducible protein 1 promotes neuritogenesis and neuroprotection by distinct signaling pathways. *J. Neurosci.* **25**, 11330–11339.

Lynch M.A. (2004). Long-term potentiation and memory. *Physiol. Rev.* **84**, 87–136.

Magalhaes A.C., Silva J.A., Lee K.S., Martins V.R., Prado V.F., Ferguson S.S., Gomez M.V., Brentani R.R., and Prado M.A. (2002). Endocytic intermediates involved with the intracellular trafficking of a fluorescen cellular prion protein. *Biol. Chem.* **277**, 33311–33318.

Maglio L.E., Perez M.F., Martins V.R., Brentani R.R., and Ramirez O.A. (2004). Hippocampal synaptic plasticity in mice devoid of cellular prion protein. *Brain Res. Mol.* **131**, 58–64.

Mallucci G.R., Ratté S., Asante E.A., Linehan J., Gowland I., Jefferys J.G.R., and Collinge J. (2002). Post-natal knockout of prion protein alters hippocampal CA1 properties, but does not result in neurodegeneration. *EMBO J.* **21**, 202–210.

Manson J.C., Clarke A.R., Hooper M.L., Aitchison L., McConnell I., and Hope J. (1994). 129/Ola mice carrying a null mutation in PrP that abolishes mRNA production are developmentally normal. *Mol. Neurobiol.* **8**, 121–127.

Manson J.C., Hope J., Clarke A.R., Johnston A., Black C., and MacLeod N. (1995). PrP gene dosage and long term potentiation. *Neurodegeneration* **4**, 113–114.

Manzerra P., Wang X.Q., Strasser U., Yu S.P., Choi D.W., and Behrens M.M. (2002). Metabotropic glutamate receptor 1-induced upregulation of NMDA receptor current: mediation through the Pyk2/Src-family kinase pathway in cortical neurons. *J. Neurosci.* **22**, 5452–5461.

Marsault R., Murgia M., Pozzan T., and Rizzuto R. (1997). Domains of high Ca2+ beneath the plasma membrane of living A7r5 cells. *EMBO J.* **16**, 1575–1581.

Mattson M.P. (2007). Calcium and neurodegeneration. *Aging Cell.* **6**, 337–350.

Mattson M.P., and Chan S.L. (2003). Neuronal and glial calcium signaling in Alzheimer's disease. *Cell Calcium* **34**, 385–397.

McKnight S., and Tjian R. (1986). Transcriptional selectivity of viral genes in mammalian cells. *Cell* **46**, 795–805.

Meyer R.K., Mckinley M.P., Bowman K.A., Braunfeld M.B., Barry R.A., and Prusiner S.B. (1986). Separation and properties of cellular and scrapie prion proteins. *Proc. Natl. Acad. Sci. USA* **83**, 2310–2314.

Miura T., Hori-i A., and Takeuchi H. (1996). Metal-dependent alpha-helix formation promoted by the glycine-rich octapeptide region of prion protein. *FEBS Letters* **396**, 248–252.

Montero M., Brini M., Marsault R., Alvarez J., Sitial R., Pozzan T., and Rizzuto R. (1995). Monitoring dynamic changes in free Ca2+ concentration in the endoplasmic reticulum of intact cells. *EMBO J.* **14**, 5467–5475.

Muramoto T., Kitamoto T., Koga H., and Tateishi J. (1992). The coexistence of Alzheimer's disease and Creutzfeldt-Jakob disease in a patient with dementia of long duration. *Acta Neuropathol.* **84**, 686–689.

Nakazawa T., Komai S., Tezuka T., Hisatsune C., Umemori H., Semba K., Mishina M., Manabe T., and Yamamoto T. (2001). Characterization of Fyn-mediated tyrosine phosphorylation sites on GluR epsilon 2 (NR2B) subunit of the N-methyl-D-aspartate. *J. Biol. Chem.* **276**, 693–699.

Nazor K.E., Seward T., and Telling G.C. (2007). Motor behavioral and neuropathological deficits in mice deficient for normal prion protein expression. *Biochim. Biophys. Acta* **1772**, 645–653.

Nedergaard M., Takano T., and Hansen A.J. (2002). Beyond the role of glutamate as a neurotransmitter. *Nature* **3**, 748–755.

Niswender C.M., and Conn P.J. (2010). Metabotropic glutamate receptors: physiology, pharmacology, and disease. *Annu. Rev. Pharmacol. Toxicol.* **50**, 295–322.

Oesch B., Westaway D., Wälchli M., McKinley M.P., Kent S.B., Aebersold R., Barry R.A., Tempst P., Teplow D.B., Hood L.E., Prusiner S.B., and Weissmann C. (1985). A cellular gene encodes scrapie PrP 27-30 protein. *Cell* **40**, 735–746.

Oidtmann B., Simon D., Holtkamp N., Ho R., and Baier M. (2003). Identification of cDNAs from Japanese pufferfish (Fugu rubripes) and Atlantic salmon (Salmo salar) coding for homologues to tetrapod prion proteins. *FEBS Lett.* **538**, 96–100.

Owen F., Poulter M., Shah T., Collinge J., Lofthouse R., Baker H., Ridley R., McVey J., Crow T.J., Risby D., Baker H.F., Ridley R.M., Hsiao K., and Prusiner S.B. (1989). Insertion in prion protein gene in familial Creutzfeldt-Jakob disease. *Lancet* **1**, 51–52.

Pan K., Baldwin M., Nguyen J., Gasset M., Serban A., Groth D., Mehlhorn I., Huang Z., Fletterick R.J., Cohen F.E., and Prusiner S.B. (1993). Conversion of alpha-helices into beta-sheets features in the formation of the scrapie prion proteins. *Proc. Natl. Acad. Sci. USA* **90**, 10962–10966.

Parekh A.B., and Putney J.J.W. (2005). Store-operated calcium channels. *Physiol. Rev.* **85**, 757–810.

Parkin E.T., Watt N.T., Hussain I., Eckman E.A., Eckman C.B., Manson J.C., Baybutt H.N., Turner A.J., and Hooper N.M. (2007). Cellular prion protein regulates beta-secretase cleavage of the Alzheimer's amyloid precursor protein. *Proc. Natl. Acad. Sci. USA* **104**, 11062–11067.

Peggion C., Bertoli A., and Sorgato M.C. (2011). Possible role for Ca2+ in the pathophysiology of the prion protein? *BioFactors* **37**, 241–249.

Powell A.D., Toescu E.C., Collinge J., and Jefferys J.G. (2008). Alterations in Ca2 + -buffering in prion-null mice: association with reduced afterhyperpolarizations in CA1 hippocampal. *J. Neurosci.* **28**, 3877–3886.

Pozo-Guisado E., Campbell D.G., Deak M., Álvarez-barrientos A., Morrice N.A., Álvarez I.S., Alessi D.R., and Martín-romero F.J. (2010). Phosphorylation of STIM1 at ERK1/2 target sites modulates store-operated calcium entry. *J. Cell Science* **123**, 3084–3093.

Prusiner S.B. (1982). Novel proteinaceous infectious particles cause scrapie. *Science* **216**, 136–144.

Prusiner S.B. (1998). Prions. *Proc. Natl. Acad. Sci. USA* **95**, 13363–13383.

Prusiner S.B., Groth D.F., Bolton D.C., Kent S.B., and Hood L.E. (1984). Purification and structural studies of a major scrapie prion protein. *Cell* **38**, 127–134.

Ramos J.W. (2008). The regulation of extracellular signal-regulated kinase (ERK) in mammalian cells. *Int. J. Biochem. Cell. Biol.* **40**, 2707–2719.

Resenberger U.K., Harmeier A., Woerner A.C., Goodman J.L., Müller V., Krishnan R., Vabulas R.M., Kretzschmar H.A., Lindquist S., Hartl F.U., Multhaup G., Winklhofer K.F., and Tatzelt J. (2011). The cellular prion protein mediates neurotoxic signalling of β-sheet-rich conformers independent of prion replication. *EMBO J.* **30**, 2057–2070.

Riek R., Hornemann S., Wider G., Billeter M., Glockshuber R., and Wüthrich K. (1996). NMR structure of the mouse prion protein domain PrP(121–231). *Nature* **382**, 180–182.

Rizzuto R., Brini M., Murgia M., and Pozzan T. (1993). Microdomains with high Ca2+ close to IP3-sensitive channels that are sensed by neighboring mitochondria. *Science* **262**, 744–747.

Rizzuto R., Simposon A.W.M., Brini M., and Pozzan T. (1992). Rapid changes of mitochondrial Ca2+ revealed by specifically targeted recombinant aequorin. *Nature* **358**, 325–327.

Rushworth J.V., and Hooper N.M. (2010). Lipid rafts: linking Alzheimer's amyloid-β production, aggregation, and toxicity at neuronal membranes. *Int. J. Alzh. Dis.* **2011**, 1–14.

Saborio G.P., Permanne B., and Soto C. (2001). Sensitive detection of pathological prion protein by cyclic amplication of protein misfolding. *Nature* **411**, 811–813.

Sah P., and Davies P. (2000). Calcium-activated potassium currents in mammalian neurons. *Clin. Exp. Pharmacol. Physiol.* **27**, 657–663.

Sandberg M.K., Al-doujaily H., Sharps B., Clarke A.R., and Collinge J. (2011). Prion propagation and toxicity in vivo occur in two distinct mechanistic phases. *Nature* **470**, 540–542.

Schägger H. (2006). Tricine-SDS-PAGE. *Nature Protocols* **1**, 16–22.

Simonic T., Duga S., Strumbo B., Asselta R., Ceciliani F., and Ronchi S. (2000). cDNA cloning of turtle prion protein. *FEBS Lett.* **469**, 33–38.

Sorgato M.C., Peggion C., and Bertoli A. (2009). Is, indeed, the prion protein a Harlequin servant of "'many'" masters? *Prion* **3**, 202–205.

Soto C. (2003). Unfolding the role of protein misfolding in neurodegenerative diseases. *Nature Rev.|Neurosc.* **4**, 49–60.

Soto C. (2011). Prion hypothesis: the end of the controversy? *Trends Biochem. Sci.* **36**, 151–158.

Sparkes R.S., Simont M., Cohntt V.H., Fournier R.E.K., Lem J., Klisak I., Heinzmann C., Blattt C., Lucero M., Mohandas T., Dearmondii S.J., Westaway D., Prusiner S.B., and Weiner L.P. (1986). Assignment of the human and mouse prion protein genes to homologous chromosomes. *Proc. Natl. Acad. Sci. USA* **83**, 7358–7362.

Stahl N., Baldwin M.A., Teplow D.B., Hood L., Gibson B.W., Burlingame A.L., and Prusiner S.B. (1993). Structural studies of the scrapie prion protein using mass spectrometry and amino acid sequencing. *Biochemistry* **32**, 1991–2002.

Stahl N., Borchelt D.R., Hsiao K., and Prusiner S.B. (1987). Scrapie prion protein contains a phosphatidylinositol glycolipid. *Cell* **51**, 229–240.

Stella R., Massimino M.L., Sandri M., Sorgato M.C., and Bertoli A. (2010). Cellular prion protein promotes regeneration of adult muscle tissue. *Mol. Cell. Biol.* **30**, 4864–4876.

Strumbo B., Ronchi S., Bolis L.C., and Simonic T. (2001). Molecular cloning of the cDNA coding for Xenopus laevis prion protein. *FEBS Lett.* **508**, 170–174.

Suzuki T., and Okumura-Noji K. (1995). NMDA receptor subunits epsilon 1 (NR2A) and epsilon 2 (NR2B) are substrates for Fyn in the postsynaptic density fraction isolated from the rat brain. *Biochem. Biophys. Res. Commun.* **216**, 582–588.

Takemura H., Hughes A.R., Thastrup O., and Putney J.W. (1989). Activation of calcium entry by the tumor promoter thapsigargin in parotid acinar cells. Evidence that an intracellular calcium pool and not an inositol phosphate regulates calcium fluxes. *J. Biol. Chem.* **264**, 12266–12271.

Tateishi J., Kitamoto T., Hoque M.Z., and Furukawa H. (1996). Experimental transmission of Creutzfeldt-Jakob disease and related diseases to rodents. *Neurology* **46**, 532–537.

Taylor D.R., and Hooper N.H. (2006). The prion protein and lipid rafts. *Mol. Membr. Biol.* **23**, 89–99.

Telling G.C., Parchi P., DeArmond S.J., Cortelli P., Montagna P., Gabizon R., Mastrianni J., Lugaresi E., Gambetti P., and Prusiner S.B. (1996). Evidence for the conformation of the pathologic isoform of the prion protein enciphering and propagating prion diversity. *Science* **274**, 2079–2082.

Traynelis S.F., Wollmuth L.P., McBain C.J., Menniti F.S., Vance K.M., Ogden K.K., Hansen K.B., Yuan H., Myers S.J., and Dingledine R. (2010). Glutamate receptor ion channels: structure, regulation, and function. *Pharmacol. Rev.* **62**, 405–496.

Um J.W., Nygaard H.B., Heiss J.K., Kostylev M.A., Stagi M., Vortmeyer A., Wisniewski T., Gunther E.C., and Strittmatter S.M. (2012). Alzheimer amyloid-β oligomer bound to postsynaptic prion protein activates Fyn to impair neurons. *Nat. Neurosci.* **15**, 1227–1235.

Varnai P., Hunyady L., and Balla T. (2009). STIM and Orai: the longawaited constituents of store-operated calcium entry. *Trends Pharmacol. Sci.* **30**, 118–128.

Voigtländer T., Klöppel S., Birner P., Jarius C., Flicker H., Verghese-Nikolakaki S., Sklaviadis T., Guentchev M., and Budka H. (2001). Marked increase of neuronal prion protein

immunoreactivity in Alzheimer's disease and human prion diseases. *Acta Neuropath.* **101**, 471–423.

Walsh D.M., Klyubin I., Fadeeva J.V., Cullen W.K., Anwyl R., Wolfe M.S., Rowan M.J., and Selkoe D.J. (2002). Naturally secreted oligomers of amyloid beta protein potently inhibit hippocampal long-term potentiation in vivo. *Nature* **416**, 535–539.

You H., Tsutsui S., Hameed S., Kannanayakal T.J., Chen L., Xia P., Engbers J.D., Lipton S.A., Stys P.K., and Zamponi G.W. (2012). Aβ neurotoxicity depends on interactions between copper ions, prion protein, and N-methyl-D-aspartate receptors. *Proc. Natl. Acad. Sci. USA* **109**, 1737–1742.

Younan N.D., Klewpatinond M., Davies P., Ruban A.V., Brown D.R., and Viles J.H. (2011). Copper (II)-induced secondary structure changes and reduced folding stability of the prion protein. *J. Mol. Biol.* **410**, 369–382.

Zahn R., Liu A., Lührs T., Riek R., Schroetter C., Lopez G.F., Billeter M., Calzolai L., Wider G., and Wüthrich K. (2000). NMR solution structure of the human prion protein. *Proc. Natl. Acad. Sci. USA* **97**, 145–150.

Zanata S.M., Lopes M.H., Mercadante A.F., Hajj G.N., Chiarini L.B., Nomizo R., Freitas A.R., Cabral A.L., Lee K.S., Juliano M.A., De Oliveira E., Jachieri S.G., Burlingame A., Huang L., Linden R., Brentani R.R., and Martins V.R. (2002). Stress-inducible protein 1 is a cell surface ligand for cellular prion that triggers neuroprotection. *EMBO J.* **21**, 3307–3316.

Zarranz J.J., Digon A., Atarés B., Rodríguez-Martínez A.B., Arce A., Carrera N., Fernández-Manchola I., Fernández-Martínez M., Fernández-Maiztegui C., Forcadas I., Galdos L., Gómez-Esteban J.C., Ibáñez A., Lezcano E., López de Munain A., Martí-Massó J.F., Mendibe M.M., Urtasun M., Uterga J.M., Saracibar N., Velasco F., and Pancorbo M.M. (2005). Phenotypic variability in familial prion diseases due to the D178N mutation. *J. Neurol. Neurosurg. Psychiatry* **76**, 1491–1496.

Zhang C.C., Steele A.D., Lindquist S., and Lodish H.F. (2006). Prion protein is expressed on long-term repopulating hematopoietic stem cells and is important for their self-renewal. *Proc. Natl. Acad. Sci. USA* **103**, 2184–2189.

Zou W.Q., Xiao X., Yuan J., Puoti G., Fujioka H., Wang X., Richardson S., Zhou X., Zou R., Li S., Zhu X., McGeer P.L., McGeehan J., Kneale G., Rincon-Limas D.E., Fernandez-Funez P., Lee H., Smith M.A., Petersen R.B., and Guo J. (2011). Amyloid-beta42 interacts mainly with insoluble prion protein in the Alzheimer brain. *J. Biol. Chem.* **286**, 15095–15105.